

# Intersecting brane world models from D8-branes on $(T^2 \times T^4/\mathbb{Z}_3)/\Omega\mathcal{R}_1$ type IIA orientifolds

**Gabriele Honecker**

*Physikalisches Institut, Universität Bonn  
Nussallee 12, D-53115 Bonn, Germany*

## Abstract

We present orientifold models of type IIA string theory with D8-branes compactified on a two torus times a four dimensional orbifold. The orientifold group is chosen such that one coordinate of the two torus is reversed when applying worldsheet parity. RR tadpole cancellation requires D8-branes which wrap 1-cycles on the two torus and transform non-trivially under the orbifold group. These models are T-dual to orientifolds with D4-branes only which admit large volume compactifications. The intersections of the D8-branes are chosen in such a way that supersymmetry is broken in the open string sector and chiral fermions arise. Stability of the models is discussed in the context of NSNS tadpoles. Two examples with the SM gauge group and two left-right symmetric models are given.

# 1 Introduction

If string theory is to be the underlying fundamental theory which unifies gravity and the gauge interactions, low energy configurations containing the standard model are expected to exist. For a long time,  $N = 1$  supersymmetric compactifications on Calabi-Yau-threefolds of the ten dimensional heterotic string seemed to be the best candidates. Some years ago, the situation started to change due to the discovery of orientifold planes [1] and the concept of D-branes [2] as end points of open strings which support the gauge groups. With this discovery, the heterotic string lost its role as the unique provider of phenomenologically interesting models. The tools of obtaining the effective lower dimensional theories from orientifold constructions were successively worked out [3, 4].

An appealing feature of type II orientifold constructions is the possibility of explaining the hierarchy between the electroweak scale  $M_Z$  and the Planck scale  $M_P$  in a natural way by taking the internal volume transverse to the D-branes to be large. By this means, the string scale can be lowered down to the TeV range [5].

Four dimensional orientifold constructions of type II superstring theories are determined by two major ingredients: Generically, the compact space is considered to be an orbifold which is a singular limit of a Calabi-Yau-threefold or  $K3$  times a two torus. Depending on the choice of the orbifold, either a quarter or half of the original supersymmetries are preserved. In addition, worldsheet parity in combination with some spacetime action can be gauged. This gauging breaks another half of the original supersymmetries. The geometric objects which are invariant under the combined action of the orbifold and worldsheet parity are called orientifold planes (O-planes). They can be transversal to some of the compact dimensions and carry RR charges. Consistency of the theory requires that RR charges are cancelled by additional objects, the D-branes. They have the same dimensionality as the O-planes. If the D-branes and O-planes are situated on top of each other in the compact space, the supersymmetry breaking is completely governed by the orbifold and worldsheet parity. The resulting models have  $\mathcal{N} = 1$  or  $\mathcal{N} = 2$  supersymmetry in the closed string as well as the open string sector. If on the other hand the D-brane data do not exactly match the O-plane data, supersymmetry can be completely broken in the open string sector while the closed sector remains  $\mathcal{N} = 1$  or  $\mathcal{N} = 2$  supersymmetric. Various realisations of the different scenarios have been studied e.g. in [6, 7, 8, 9, 10].

One possible way to realise the supersymmetry breaking in the open string sector is given by including not only D-branes but also anti-D-branes in the models. Strings stretching between a brane and an anti-brane have masses depending on the distance between these branes. For small distances, tachyons occur in the spectrum which render the theory unstable and induce a phase transition [11, 12].

Another way of breaking supersymmetry in the open string sector of type II orientifolds is to allow for a non-trivial magnetic background flux in torus compactifications [13, 14]. These fluxes can also trigger gauge and chiral symmetry breaking. In a T-dual picture, the magnetic background fluxes are described by relative angles of intersecting D-branes which wrap different cycles in the compact space [15, 16]. In this picture, massless chiral fermions are supported at the intersection loci of two D-branes [17]. Tilting the compactification torus in this picture corresponds to including a non-trivial discrete NSNS-sector B field in the T-dual picture with magnetic background fluxes [18, 19]. The effect of this is a further gauge symmetry breaking as well as a change in the number of generations. Such supersymmetry breaking four dimensional orientifold models with D6-branes at angles on tori and some orbifolds have also been considered in [20, 21, 22, 23], and in [24] a particular subclass of such models was discovered where by choosing special intersection angles, chiral symmetry is broken but supersymmetry is preserved.

In [25, 26, 27] the picture of branes at angles was examined within the framework of type II superstring theory on a four dimensional orbifold. Upon compactifying on an additional two torus, D4-branes sitting at the orbifold fixed points can intersect.

In this paper, we consider a hybrid ansatz of the previously discussed ones. We construct orientifold models of type II superstring theory on a four dimensional orbifold times a two torus. The orientifold group is chosen such that D8-branes are required for tadpole cancellation. These D8-branes wrap a non-trivial cycle on the two torus while they fill the non-compact space and the orbifold. The orbifold group acts non trivially on the Chan-Paton factors of the open strings leading to a classification of representations of chiral fermions according to the transformation properties of their groundstates under the orbifold group. These models have a T-dual description in terms of D4-branes and thus constitute the orientifolded version of the models constructed in [25] which admit large volume compactifications. One particular example of these models has already been presented in [28]. While preparing the manuscript, the letter article [29] appeared where also intersecting D4-branes in an unoriented theory are briefly mentioned.

The paper is organized as follows. In section 2, we present the construction of type II orientifold models with D8-branes at angles. This includes the computation of RR tadpoles and the generic chiral open spectrum. In section 3, we comment on the Green-Schwarz mechanism required for cancellation of mixed anomalies. In section 4, we discuss the stability of our models in terms of NSNS tadpoles. In section 5, we present two models with four generations and the standard model gauge group as well as two left-right symmetric models with three generations. The last section 6, is devoted to a discussion and conclusions. Finally, details of the calculation are accumulated in the appendices A, B, C and D.

## 2 Construction of $(T^2 \times T^4/Z_3)/\Omega\mathcal{R}_1$ Orientifolds

### 2.1 General Setup

In this article we discuss four dimensional orientifold models of type IIA theory on  $T^2 \times T^4/Z_3$  with D8-branes at angles. The four non-compact dimensions are labeled by  $x^\mu$ ,  $\mu = 0, \dots, 3$ . The compact space can be parameterized by three complex coordinates,

$$z^1 = x^4 + ix^5, \quad z^2 = x^6 + ix^7, \quad z^3 = x^8 + ix^9. \quad (1)$$

corresponding to three two tori  $T_{1,2,3}$ . In the model under consideration, worldsheet parity  $\Omega$  is combined with a reflexion on the first two torus,

$$\mathcal{R}_1 : z^1 \rightarrow \bar{z}^1, \quad (2)$$

and the generator  $\Theta$  of  $\mathbb{Z}_3$  acts on the second and third torus,

$$\Theta : z^i \rightarrow e^{2\pi i v_i} z^i, \quad (3)$$

with  $v = (0, 1/3, -1/3)$ . The sets of points which are left invariant under  $\Omega\mathcal{R}_1 \times \Theta$  constitute orientifold planes, which are extended along all non-compact directions and the four dimensional orbifold, but only along the  $x^4$  axis on the first torus. Thus, they extend along eight spatial dimensions. In order to cancel the RR-charges of these O8-planes, an appropriate configuration of D8-branes has to be added. Performing a T-duality along the  $x^5$  direction, D8-branes at angles on  $T_1$  correspond to D9-branes with non-trivial magnetic background flux  $F$  which is quantized in terms of the radii of the two-torus,  $F = \frac{\alpha'}{R_1 R_2} \frac{q}{p}$  [16, 15]. In addition, toroidal compactifications of type I string theory allow for a non-trivial constant background NSNS two-form flux  $b = 0, 1/2$  [30]. In the T-dual picture with D8-branes at angles, the discrete value  $b = 1/2$  corresponds to a tilted torus lattice w.r.t. the real axis as discussed in [19] or the **b** type lattice of [23]. The relation between these two ways of describing the torus is explicitly shown in appendix A.2. D8<sub>a</sub>-branes are specified by the wrapping numbers  $(n_a, m_a)$  along the two fundamental cycles of  $T_1$ . In the T-dual picture with D9-branes, these wrapping numbers are replaced by the quantization condition

on the magnetic and the NSNS background flux, i.e.  $(p_a, q_a) \simeq (n_a, m_a + bn_a)$ . Due to the reflexion symmetry  $\mathcal{R}_1$ , each  $D8_a$ -brane is accompanied by its mirror image  $D8'_a$  with wrapping numbers  $(n'_a, m'_a) = (n_a, -m_a - 2bn_a)$ . Two stacks of branes  $D8_a$  and  $D8_b$  generically have several intersections within the fundamental cell of the torus. The corresponding intersection numbers can be expressed in terms of the wrapping numbers,

$$I_{ab} = n_a m_b - n_b m_a. \quad (4)$$

Formally, the intersection number can take negative values. In terms of physical quantities, this means that the particles with support at the intersection locus transform under the conjugate representation. In the model under consideration, the orbifold generator  $\Theta$  preserves the position of each  $D8_a$  brane while assigning different phases  $\alpha^j$  (where  $\alpha \equiv e^{2\pi i/3}$  and  $j = 0, 1, 2$ ). Therefore, a stack of  $N_a$  branes with identical positions is decomposed according to the different eigenvalues of the  $\mathbb{Z}_3$  rotation,  $N_a = N_a^0 + N_a^1 + N_a^2$ , giving rise to the gauge group

$$U(N_a^0) \times U(N_a^1) \times U(N_a^2). \quad (5)$$

Particles which are supported at the intersection locus of two stacks of branes  $D8_a$  and  $D8_b$  with  $\mathbb{Z}_3$  eigenvalue 1 transform as  $(N_a^i, \bar{N}_b^i)$  whereas those with eigenvalue  $\alpha^{\pm 1}$  transform as  $(N_a^i, \bar{N}_b^{i\pm 1})$ .

The gauge coupling constants of the  $U(N_a^i)$  factors with support on a  $D8_a$  brane are determined by the length  $L_a$  of the 1-cycle on  $T_1$  which the  $D8_a$  brane wraps [26],

$$\frac{2\pi}{g_a^2} \sim \frac{M_s}{\lambda_s} L_a. \quad (6)$$

The length of the cycle in terms of wrapping numbers and radii of the two-torus is given by

$$L_a = \sqrt{(n_a R_1)^2 + ((m_a + bn_a) R_2)^2}. \quad (7)$$

In this class of models, Yukawa couplings arise from bosonic and fermionic fields living at the intersection loci of three different types of  $D8_{a,b,c}$  branes. These intersection points constitute the cusps of a triangle of area  $A_{abc}$  (which is dimensionless when the area of the torus  $T_1$  is measured in string units). The size of Yukawa couplings is exponentially suppressed in terms of the area [26],

$$Y_{abc} = \exp(-A_{abc}). \quad (8)$$

## 2.2 RR-Tadpole Cancellation

In this section, we derive the consistency conditions of the  $(T^2 \times T^4/\mathbb{Z}_3)/\Omega\mathcal{R}_1$  models which are determined by the requirement that all – untwisted and twisted – RR-charges of the O8-planes are cancelled by those of the  $D8_a$ -branes. These so called tadpole cancellation conditions can be entirely expressed in terms of the wrapping numbers  $n_a$  corresponding to the projection onto the  $x^4$ -axis and the number of identical branes  $N_a^i$ .

In the closed string sector at 1-loop, the Klein-bottle amplitude contributes to the RR-tadpole. This divergence can be cancelled by the two 1-loop amplitudes of the open string sector, namely the annulus and the Möbius strip. The 1-loop amplitudes are depicted in figure 1 where time  $t$  evolves along the vertical direction. By choosing the time  $l$  to run along the horizontal direction instead, one obtains the picture in the tree-channel where the Klein bottle amplitude is given by a closed string scattered between two O8-planes, the annulus by scattering between a  $D8_a$  and a  $D8_b$ -brane and the Möbius strip between a  $D8_a$ -brane and an O8-plane. The O8-planes are described by crosscap states invariant under  $\Omega\mathcal{R}_1 h$  where  $g, h$  label elements of the orbifold group  $\mathbb{Z}_N$ .  $g$

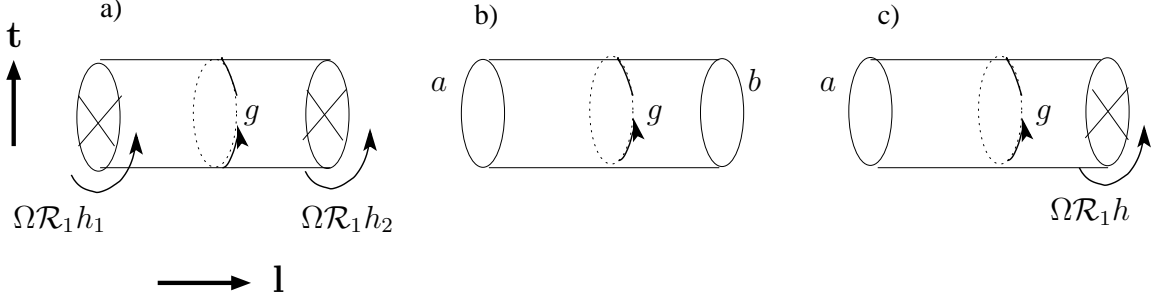


Figure 1: a) Klein bottle, b) Annulus, c) Möbius strip

denotes the twist sector of the closed string propagating in the tree-channel. Consistency of the boundary conditions requires in the Klein bottle diagram [4]

$$(\Omega\mathcal{R}_1 h_1)^2 = (\Omega\mathcal{R}_1 h_2)^2 = g \quad (9)$$

and in the Möbius strip

$$(\Omega\mathcal{R}_1 h)^2 = g. \quad (10)$$

In contrast to the models with branes at angles considered in [10, 22, 23], the following relation holds

$$(\Omega\mathcal{R}_1 h)^2 = h^2. \quad (11)$$

Therefore, twisted as well as untwisted closed strings propagate in the tree channel leading to untwisted and twisted tadpole cancellation conditions which have to be fulfilled simultaneously.

At this point, we turn to the explicit calculation of the three 1-loop-amplitudes. The direct calculation in the tree-channel can be performed using the boundary state approach (see e.g. [12]). For our class of models, the relevant formulas are displayed in appendix B. The constraints on  $N_a^i$  can, however, only be read off by starting from the 1-loop amplitudes.

### 2.2.1 Klein bottle

The closed string 1-loop contribution to the RR-exchange in the tree-channel can be obtained by computing the NSNS part with  $(-1)^F$  insertion (where  $F$  is the worldsheet fermion number). The lattice contributions  $\mathcal{L}_1$  on  $T_1$  where the reflexion  $\mathcal{R}_1$  acts are as discussed in [19, 23]. In addition, in the untwisted sector Kaluza Klein momenta arise along all directions of the orbifold whereas windings are projected out by worldsheet parity. The explicit formulas for the lattice contributions of the orbifold to the amplitudes are listed in appendix A.1.  $\Omega\mathcal{R}_1$  exchanges  $\Theta$  and  $\Theta^{-1}$  twisted sectors. Hence, in the 1-loop channel, only untwisted sectors contribute. The calculation of the contribution with  $\mathbb{1}$  insertion goes completely along the lines discussed in [19, 23] yielding

$$\mathcal{K}_U = \frac{c}{3} \int_0^\infty \frac{dt}{t^3} \mathcal{L}_1^\mathcal{K} \mathcal{L}_2^\mathcal{K} \mathcal{L}_3^\mathcal{K} \mathcal{K}^{(0)} \quad (12)$$

where  $c \equiv V_4/(8\pi^2\alpha')^2$  contains the regularized four dimensional volume  $V_4$  arising from integrating out the non-compact momenta.  $\mathcal{L}_2^\mathcal{K} \mathcal{L}_3^\mathcal{K}$  is as given in (67) in appendix A.1. Performing the modular transformation  $t = 1/(4l)$  gives the contribution from the untwisted RR-fields,

$$\mathcal{K}^U = \frac{c}{3} \int_0^\infty dl \frac{256}{3} \frac{R_1}{R_2} \omega \tilde{\mathcal{L}}_1^\mathcal{K} \tilde{\mathcal{L}}_2^\mathcal{K} \tilde{\mathcal{L}}_3^\mathcal{K} \tilde{\mathcal{K}}^{(0)}. \quad (13)$$

where  $R_{1,2}$  are the two radii of the first two-torus  $T_1$  and  $\omega$  is the volume of the orbifold  $T^4/\mathbb{Z}_3$ .

In addition,  $\Theta^{1,2}$  insertions create tadpoles which are independent of the internal volume of the orbifold,

$$\mathcal{K}^T = \frac{c}{3} \int_0^\infty \frac{dt}{t^3} \mathcal{L}_1^\mathcal{K} \sum_{k=1}^2 \mathcal{K}^{(k)}. \quad (14)$$

The explicit expression of  $\mathcal{K}^{(k)}$  in terms of generalized Jacobi-Theta functions is given in formula (73) in appendix A.4. The lattice contributions  $\mathcal{L}_1^\mathcal{K}$  are the same as in formula (12), whereas the Kaluza Klein momenta on  $T_{2,3}$  are not invariant under  $\Theta$ . Transforming to the tree channel, the twisted Klein bottle is given by

$$\mathcal{K}^T = -16 \frac{c}{3} \int_0^\infty dl \frac{R_1}{R_2} \tilde{\mathcal{L}}_1^\mathcal{K} \sum_{k=1}^2 \tilde{\mathcal{K}}^{(k)} \quad (15)$$

where  $\tilde{\mathcal{K}}^{(k)}$  is given by (76) in appendix A.4.

### 2.2.2 Annulus

The annulus amplitude is obtained from open strings stretching between branes  $D8_a$  and  $D8_b$  at angle  $\pi\Delta\varphi_{ab}$  on  $T_1$ . The contributions from  $T_1$  have been discussed in detail in [19, 23]. The computation of the trace with trivial insertion is again completely analogous to the one performed in [19, 23] yielding the untwisted RR-tadpole of the annulus in the tree-channel

$$\mathcal{A}_{ab}^U = -N_a N_b I_{ab} \frac{c}{3} \int_0^\infty dl \frac{1}{6} \omega \tilde{\mathcal{A}}^{(0)} \tilde{\mathcal{L}}_2^{\mathcal{A}} \tilde{\mathcal{L}}_3^{\mathcal{A}}. \quad (16)$$

$N_a$  labels the number of  $D8_a$  branes of identical position,  $I_{ab}$  is the intersection number on  $T_1$  defined in (4),  $\tilde{\mathcal{L}}_2^{\mathcal{A}} \tilde{\mathcal{L}}_3^{\mathcal{A}}$  is given in (68) in appendix A.1 and the oscillator contribution is given by

$$\tilde{\mathcal{A}}^{(0)} = \frac{\vartheta \begin{bmatrix} 1/2 \\ 0 \end{bmatrix}^3}{\eta^9} \frac{\vartheta \begin{bmatrix} 1/2 \\ \Delta\varphi \end{bmatrix}}{\vartheta \begin{bmatrix} 1/2 \\ 1/2 + \Delta\varphi \end{bmatrix}} (2l) \xrightarrow{l \rightarrow \infty} \frac{-8}{I_{ab}} \left( n_a n_b \frac{R_1}{R_2} + (m_a + b n_a)(m_b + b n_b) \frac{R_2}{R_1} \right). \quad (17)$$

The explicit dependence of the annulus tadpole on the orbifold volume  $\omega$  is due to the fact that  $D8_a$  branes have Neumann directions along  $x^{6\dots 9}$  leading to Kaluza Klein momenta  $p^{6\dots 9}$ .

In addition to the trivial insertion, each  $\Theta^k$  insertion preserves the positions of branes. Kaluza Klein momenta are projected out, and the  $\mathbb{Z}_3$  rotation acts non-trivially on the Chan-Paton labels of the open string with endpoints on branes  $a, b$  via the matrices  $\gamma_{\Theta^k}^a, \gamma_{\Theta^k}^b$  leading to

$$\mathcal{A}_{ab}^T = \frac{I_{ab} c}{4} \frac{1}{3} \int_0^\infty \frac{dt}{t^3} \sum_{k=1}^2 \text{tr} \gamma_k^a \text{tr} \gamma_k^{-1,b} \mathcal{A}^{(k)} \quad (18)$$

with  $\mathcal{A}^{(k)}$  explicitly listed in (74) in appendix A.4. By modular transformation  $t = 1/(2l)$ , one arrives at the twisted RR-tadpole contribution of the annulus,

$$\mathcal{A}_{ab}^T = -I_{ab} \frac{c}{3} \int_0^\infty dl \frac{1}{2} \sum_{k=1}^2 \text{tr} \gamma_k^a \text{tr} \gamma_k^{-1,b} \tilde{\mathcal{A}}^{(k)} \quad (19)$$

with  $\tilde{\mathcal{A}}^{(k)}$  given by (77) in appendix A.4. Thus, the asymptotic behaviour of the annulus amplitudes is given by

$$\mathcal{A}_{ab}^U \xrightarrow{l \rightarrow \infty} N_a N_b \frac{4}{3} \omega \frac{c}{3} \int_0^\infty dl \left( n_a n_b \frac{R_1}{R_2} + (m_a + b n_a)(m_b + b n_b) \frac{R_2}{R_1} \right), \quad (20)$$

$$\mathcal{A}_{ab}^T \xrightarrow{l \rightarrow \infty} -\frac{c}{3} \int_0^\infty dl \sum_{k=1}^2 \text{tr} \gamma_k^a \text{tr} \gamma_k^{-1,b} \left( n_a n_b \frac{R_1}{R_2} + (m_a + b n_a)(m_b + b n_b) \frac{R_2}{R_1} \right). \quad (21)$$

### 2.2.3 Möbius strip

The computation of the untwisted RR-exchange in the tree channel arising from the Möbius strip amplitude is again very similar to the case discussed in [19, 23]. Only strings stretching between mirror branes  $a$  and  $a'$  contribute. Their multiplicity is determined by the number of  $\Omega\mathcal{R}_1$  invariant intersections  $I_{aa'}^{\Omega\mathcal{R}_1}$  listed in appendix A.3, and the Neumann directions on  $T_{2,3}$  lead to lattice contributions from Kaluza Klein momenta displayed in (69) in appendix A. Therefore, the untwisted RR-exchange is linearly proportional to the orbifold volume  $\omega$ .

The computation of the twisted RR-tadpoles in the Möbius strip is also completely analogous to the annulus case. The  $\mathbb{Z}_3$  rotation acts non-trivially on the Chan-Paton-matrix of the  $aa'$  string, lattice contributions are projected out and the oscillator contributions are listed in (78) in appendix A.4. In summary, we obtain the asymptotic behaviour

$$\mathcal{M}_a^U \xrightarrow{l \rightarrow \infty} -\frac{c}{3} \int_0^\infty dl \frac{256}{3} \frac{R_1}{R_2} \omega n_a \text{tr} \left( \gamma_{\Omega\mathcal{R}_1}^{-1,a'} \gamma_{\Omega\mathcal{R}_1}^{T,a} \right), \quad (22)$$

$$\mathcal{M}_a^T \xrightarrow{l \rightarrow \infty} \frac{c}{3} \int_0^\infty dl 16 n_a \frac{R_1}{R_2} \sum_{k=1}^2 \text{tr} \left( \gamma_{\Omega\mathcal{R}_1 k}^{-1,a'} \gamma_{\Omega\mathcal{R}_1 k}^{T,a} \right). \quad (23)$$

The trace in (23) can be transformed due to closure of the orientifold group, i.e.

$$\gamma_{k+l}^a = c_{k+l} \gamma_{\Omega\mathcal{R}_1 l}^{l-T,a'} \gamma_{\Omega\mathcal{R}_1 k}^a. \quad (24)$$

### 2.2.4 RR-tadpole cancellation

The RR-tadpole cancellation conditions can be extracted from the asymptotic behaviour of the Klein bottle ((13) and (15)), the annulus ((16) and (19)) and the Möbius strip ((22) and (23)) after summing over all possible open string configurations.

The untwisted tadpole conditions are

$$\left[ \sum_a n_a N_a - 16 \right]^2 = 0, \quad (25)$$

$$\text{tr} \left( \gamma_{\Omega\mathcal{R}_1}^{-1,a'} \gamma_{\Omega\mathcal{R}_1}^{T,a} \right) = N_a. \quad (26)$$

The twisted tadpole conditions split into the projection onto the  $x^4$  axis proportional to  $R_1/R_2$  and to the  $x^5$  direction proportional to  $R_2/R_1$ ,

$$\frac{R_2}{R_1} : \quad \sum_{k=1}^2 \left| \sum_a (m_a + b n_a) \left( \text{tr} \gamma_k^a - \text{tr} \gamma_k^{a'} \right) \right|^2 = 0, \quad (27)$$

$$\frac{R_1}{R_2} : \quad \sum_{k=1}^2 \left( 8^2 + \left| \sum_a n_a \left( \text{tr} \gamma_k^a + \text{tr} \gamma_k^{a'} \right) \right|^2 - 2 \cdot 8 \cdot \sum_a n_a \left( c_{2k} \text{tr} \gamma_{2k}^a + \tilde{c}_{2k} \text{tr} \gamma_{2k}^{a'} \right) \right) = 0. \quad (28)$$

Condition (27) is trivially fulfilled if for mirror branes  $D8_a$  and  $D8_{a'}$  the identity  $\text{tr}\gamma_k^a = \text{tr}\gamma_k^{a'}$  holds. Furthermore, equation (28) gives a total square for each twist sector  $k$  provided that  $c_{2k} = \tilde{c}_{2k} = 1$  and  $\text{tr}\gamma_{2k} \in \mathbb{R}$ . These conditions fix the form of  $\gamma_\Theta^a$ ,

$$\gamma_\Theta^a = \text{diag} \left( \mathbb{1}_{N_a^0}, e^{2\pi i/3}, e^{-2\pi i/3} \right) \quad (29)$$

with  $N_a = N_a^0 + N_a^1 + N_a^2$  and  $N_a^1 = N_a^2$ .

Inserting (29) in (25) and (28) determines the RR-tadpole cancellation conditions entirely in terms of the wrapping numbers  $n_a$  along the  $x^4$  axis and the number of identical branes  $N_a^i$ ,

$$\sum_a n_a N_a^0 = 8, \quad (30)$$

$$\sum_a n_a N_a^1 = 4. \quad (31)$$

So far, we have only considered  $D8_a$  branes which are mapped to their mirror image  $D8_{a'}$  under the reflexion  $\mathcal{R}_1$ . A  $D8_c$  brane which is its own mirror image contributes only half the amount to the tadpole conditions, i.e.

$$\frac{n_c N_c^0}{2} + \sum_{a \neq c} n_a N_a^0 = 8, \quad (32)$$

$$\frac{n_c N_c^1}{2} + \sum_{a \neq c} n_a N_a^1 = 4. \quad (33)$$

The wrapping numbers of the  $\Omega\mathcal{R}_1$  invariant brane are  $(n_c, m_c) = (1, 0)$  for vanishing background antisymmetric NSNS tensor field  $b$  and  $(n_c, m_c) = (2, -1)$  for  $b = 1/2$ . In the limit  $R_1, \frac{1}{R_2} \rightarrow \infty$  where the T-dual two-torus  $T_1$  decompactifies, the supersymmetric six dimensional set-up is recovered which for vanishing antisymmetric NSNS tensor, i.e. a single stack of branes with  $(n_c, m_c) = (1, 0)$  and  $b = 0$ , is identical to the  $\mathbb{Z}_3$  orientifold in [7].

### 2.3 Chiral open spectrum

The closed string spectrum contains the  $\mathcal{N} = 2$  SUGRA multiplet as well as eleven hypermultiplets and ten tensor multiplets. The complete closed string sector is  $\mathcal{N} = 2$  supersymmetric and non-chiral. In order to determine the open string spectrum, we fix the Chan-Paton matrices

$$\gamma_{\Omega\mathcal{R}_1}^a = \gamma_{\Omega\mathcal{R}_1}^{a'} = \begin{pmatrix} \mathbb{1}_{N_a^0} & 0 & 0 \\ 0 & 0 & \mathbb{1}_{N_a^1} \\ 0 & \mathbb{1}_{N_a^1} & 0 \end{pmatrix}, \quad (34)$$

$$\gamma_\Theta^a = \gamma_\Theta^{a'} = \text{diag} \left( \mathbb{1}_{N_a^0}, e^{2\pi i/3}, e^{-2\pi i/3} \right) \quad (35)$$

in analogy to the supersymmetric case discussed in [7]. Open strings stretching between identical branes then give the gauge groups

$$U(N_a^0) \times (U(N_a^1))^2. \quad (36)$$

In the case of an  $\Omega\mathcal{R}_1$  invariant brane, the gauge group is reduced to

$$SO(N_a^0) \times U(N_a^1). \quad (37)$$

The  $aa$  sectors of open strings are again  $\mathcal{N} = 2$  supersymmetric and non-chiral.



Finally, the sector of  $ab$  strings stretching between  $D8_a$  and  $D8_b$  branes at angles  $\pi\Delta\varphi_{ab}$  is non-supersymmetric and chiral. This part of the spectrum generically contains tachyons since masses of states in the NS sector are given by

$$\alpha' m_{ab}^2 = \text{osc} + \frac{\Delta\varphi_{ab}}{2} - \frac{1}{2}. \quad (38)$$

Thus, the state  $\psi_{\Delta\varphi-1/2}^1|0\rangle_{NSNS}$  is tachyonic. A complete list of lightest NS states is given in appendix C. In contrast to the models with  $D6_a$  branes discussed in [23], mass eigenstates in the models with  $D8_a$  branes have to be classified according to their  $\mathbb{Z}_3$  eigenvalue. Tachyonic states only occur in the sectors with eigenvalue 1. In principle, this introduces the possibility of choosing the brane set-up, i.e. the numbers  $N_a^i$ , such that no chiral sector with trivial eigenvalue occurs. However, the tadpole conditions (32), (33) constrain the models severely. Furthermore, in contrast to the type IIB models examined in [25, 26, 27] the orientifold projection  $\Omega\mathcal{R}_1$  enforces the existence of mirror branes.  $aa'$  strings automatically include a sector containing tachyons which can be only projected out completely by the  $\Omega\mathcal{R}_1$  symmetry in case of a single  $U(1)_a$  gauge factor.

The R sector of branes at angles provides chiral fermions. The groundstate is fourfold degenerated as displayed in the table in appendix C. The degeneracy is lifted by the  $\mathbb{Z}_3$  symmetry. In summary, the chiral spectrum is listed in table 1. For an  $\Omega\mathcal{R}_1$  invariant brane  $D8_c$ , the spectrum is slightly changed as displayed in table 2. Generically, the sector  $a'b'$  provides the anti-particles of the  $ab$  sector and the sector  $ab'$  is paired with  $a'b$ . But for  $c = c'$ , only the sectors  $cb$  and  $cb'$  are present and form a pair. RR-tadpole cancellation ensures that the chiral spectrum is free of purely non-abelian gauge anomalies. Mixed  $U(1)$  anomalies will have to be cured by a generalized Green-Schwarz mechanism involving twisted RR-fields from the closed string sector [31, 25, 32].

The chiral  $aa'$ ,  $ab$  and  $ab'$  sectors with  $\mathbb{Z}_3$  eigenvalue 1 are accompanied by a tachyonic scalar. As already mentioned in the previous paragraph, the  $aa'$  sector is only absent provided that  $n_a = 1$  and  $N_a^0 = 1, N_a^1 = N_a^2 = 0$ , i.e. the  $D8_a$  brane accommodates a single  $U(1)_a$  gauge factor.

### 3 Cancellation of Mixed Anomalies

The generic chiral open spectrum displayed in table 1 and 2 is free of purely non-abelian gauge anomalies, but yields mixed gravitational anomalies of the form

$$U(1)_{i,a} - g_{\mu\nu} : 6(2\delta_{i,0} - \delta_{i,1} - \delta_{i,2})(m_a + bn_a)N_a^i \quad (39)$$

as well as mixed gauge anomalies which for  $(i, a) \neq (j, b)$  are proportional to

$$U(1)_{i,a} - SU(N_b^j)^2 : \left\{ (m_a + bn_a)n_b(2\delta_{i,0} - \delta_{i,1} - \delta_{i,2})(2\delta_{j,0} - \delta_{j,1} - \delta_{j,2}) \right. \\ \left. - 3n_a(m_b + bn_b)(\delta_{i,1} - \delta_{i,2})(\delta_{j,1} - \delta_{j,2}) \right\} N_a^i C_2(N_b^j) \quad (40)$$

where  $C_2(N) = \frac{N^2-1}{2N}$  is the quadratic Casimir of the fundamental representation of  $SU(N)$ .

Consistency of the models requires anomalous gauge fields to acquire a mass and thus decouple from the effective low energy field theory. This is realized by the Green-Schwarz mechanism which in models with  $K3$  orbifold compactifications involve twisted sector fields [31]. The potential candidates are the RR scalars  ${}^6C_k^{(0)}$  and two-forms  ${}^6C_k^{(2)}$  in six dimensions which belong to the sixdimensional twisted hyper- and tensormultiplets, respectively. They arise from the Kaluza Klein reduction of the ten-dimensional two form  ${}^{10}C^{(2)}$  and self-dual four form  ${}^{10}C^{(4)}$  on a vanishing supersymmetric two-cycle  $\Sigma_k$  on the orbifold,

$${}^6C_k^{(2)} = \int_{\Sigma_k} {}^{10}C^{(4)}, \quad {}^6C_k^{(0)} = \int_{\Sigma_k} {}^{10}C^{(2)}. \quad (41)$$

Massless chiral fermionic spectrum on $T^2 \times T^4/\mathbb{Z}_3$ with D8-branes			
sector	$\mathbb{Z}_3$	multiplicity	rep.
$aa'$	1	$2(2m_a + (2b)n_a)$	$(\mathbf{A}_a^0, 1, 1) + (1, \mathbf{F}_a^1, \mathbf{F}_a^2)$
	$\alpha$	$(n_a - 1)(2m_a + (2b)n_a)$	$(\mathbf{A}_a^0 + \mathbf{S}_a^0, 1, 1) + 2(1, \mathbf{F}_a^1, \mathbf{F}_a^2)$
		$(2m_a + (2b)n_a)$	$(\bar{\mathbf{F}}_a^0, 1, \bar{\mathbf{F}}_a^2) + (1, \bar{\mathbf{A}}_a^1, 1)$
		$\frac{n_a-1}{2}(2m_a + (2b)n_a)$	$2(\bar{\mathbf{F}}_a^0, 1, \bar{\mathbf{F}}_a^2) + (1, \bar{\mathbf{A}}_a^1 + \bar{\mathbf{S}}_a^1, 1)$
	$\alpha^2$	$(2m_a + (2b)n_a)$	$(\bar{\mathbf{F}}_a^0, \bar{\mathbf{F}}_a^1, 1) + (1, 1, \bar{\mathbf{A}}_a^2)$
		$\frac{n_a-1}{2}(2m_a + (2b)n_a)$	$2(\bar{\mathbf{F}}_a^0, \bar{\mathbf{F}}_a^1, 1) + (1, 1, \bar{\mathbf{A}}_a^2 + \bar{\mathbf{S}}_a^2)$
$ab$	1	$2(n_a m_b - n_b m_a)$	$(\bar{\mathbf{F}}_a^0, \mathbf{F}_b^0) + (\bar{\mathbf{F}}_a^1, \mathbf{F}_b^1) + (\bar{\mathbf{F}}_a^2, \mathbf{F}_b^2)$
	$\alpha$	$(n_a m_b - n_b m_a)$	$(\mathbf{F}_a^0, \bar{\mathbf{F}}_b^1) + (\mathbf{F}_a^1, \bar{\mathbf{F}}_b^2) + (\mathbf{F}_a^2, \bar{\mathbf{F}}_b^0)$
	$\alpha^2$	$(n_a m_b - n_b m_a)$	$(\mathbf{F}_a^0, \bar{\mathbf{F}}_b^2) + (\mathbf{F}_a^1, \bar{\mathbf{F}}_b^0) + (\mathbf{F}_a^2, \bar{\mathbf{F}}_b^1)$
$ab'$	1	$2(n_a m_b + n_b m_a + (2b)n_a n_b)$	$(\mathbf{F}_a^0, \mathbf{F}_b^0) + (\mathbf{F}_a^1, \mathbf{F}_b^2) + (\mathbf{F}_a^2, \mathbf{F}_b^1)$
	$\alpha$	$(n_a m_b + n_b m_a + (2b)n_a n_b)$	$(\bar{\mathbf{F}}_a^0, \bar{\mathbf{F}}_b^2) + (\bar{\mathbf{F}}_a^1, \bar{\mathbf{F}}_b^1) + (\bar{\mathbf{F}}_a^2, \bar{\mathbf{F}}_b^0)$
	$\alpha^2$	$(n_a m_b + n_b m_a + (2b)n_a n_b)$	$(\bar{\mathbf{F}}_a^0, \bar{\mathbf{F}}_b^1) + (\bar{\mathbf{F}}_a^1, \bar{\mathbf{F}}_b^0) + (\bar{\mathbf{F}}_a^2, \bar{\mathbf{F}}_b^2)$

Table 1: Chiral spectrum. The sectors are classified by the  $\mathbb{Z}_3$  eigenvalue of the corresponding R groundstate.

The scalar has a dual four form in six dimensions,

$${}^6C_k^{(4)} = \int_{\Sigma_k} {}^{10}C^{(6)}. \quad (42)$$

Modding out the worldsheet parity amounts to mapping different cycles  $\Sigma_k$  onto each other such that for the  $T^4/\mathbb{Z}_3$  limit,  $k$  runs over nine distinct values.

Reducing further down to four dimensions, the pullback of a closed sector two form on a multiply wrapped brane gives a scalar times the wrapping number along the  $\Omega\mathcal{R}_1$  invariant direction [25],

$$n_b B_k^{(0)} = \int_{T^2(D9_b)} {}^6C_k^{(2)} \quad n_b B_k^{(2)} = \int_{T^2(D9_b)} {}^6C_k^{(4)} \quad (43)$$

while integrating out the two form  $\mathcal{F}_a = F_a + B_a = \frac{(m_a + bn_a)\alpha'}{n_a R_1 R_2}$  on the torus yields as prefactor  $m_a + bn_a$ . The resulting four dimensional couplings are of the form

$$\begin{aligned} (m_a + bn_a) \int_{R^{1,3}} \text{tr}(\gamma_k^a \lambda_i^a) C_k^{(2)} \wedge F_{a,i} & \quad n_b \int_{R^{1,3}} \text{tr}(\gamma_k^b \lambda_i^b \lambda_j^b) B_k^{(0)} F_{b,i} \wedge F_{b,j} \\ n_a \int_{R^{1,3}} \text{tr}(\gamma_k^a \lambda_i^a) B_k^{(2)} \wedge F_{a,i} & \quad (m_a + bn_a) \int_{R^{1,3}} \text{tr}(\gamma_k^b \lambda_i^b \lambda_j^b) C_k^{(0)} F_{b,i} \wedge F_{b,j} \end{aligned} \quad (44)$$

where  $\lambda_i^a$  is the Chan-Paton-factor belonging to the gauge-field component  $F_{a,i}$ .

The expressions on the left hand side in (44) render the anomalous gauge fields massive. Combining the two couplings (44) of the scalars  $B_k^{(0)}$  and their dual two form  $C_k^{(2)}$ , we obtain the Green-Schwarz diagram depicted in figure 2, similarly for the dual pair  $C_k^{(0)}$  and  $B_k^{(2)}$ . These diagrams have the correct form to cancel the mixed anomalies (39) and (40).

Chiral fermions for an $\Omega\mathcal{R}_1$ invariant brane $D8_c$			
sector	$\mathbb{Z}_3$	multiplicity	rep.
$cb$	1	$2n_c(m_b + bn_b)$	$(\bar{\mathbf{F}}_c^0, \mathbf{F}_b^0) + (\bar{\mathbf{F}}_c^1, \mathbf{F}_b^1) + (\mathbf{F}_c^1, \mathbf{F}_b^2)$
	$\alpha$	$n_c(m_b + bn_b)$	$(\mathbf{F}_c^0, \bar{\mathbf{F}}_b^1) + (\mathbf{F}_c^1, \bar{\mathbf{F}}_b^2) + (\bar{\mathbf{F}}_c^1, \bar{\mathbf{F}}_b^0)$
	$\alpha^2$	$n_c(m_b + bn_b)$	$(\mathbf{F}_c^0, \bar{\mathbf{F}}_b^2) + (\mathbf{F}_c^1, \bar{\mathbf{F}}_b^0) + (\bar{\mathbf{F}}_c^1, \bar{\mathbf{F}}_b^1)$

Table 2: Modification of the chiral spectrum involving an  $\Omega\mathcal{R}_1$  invariant brane  $c$ .

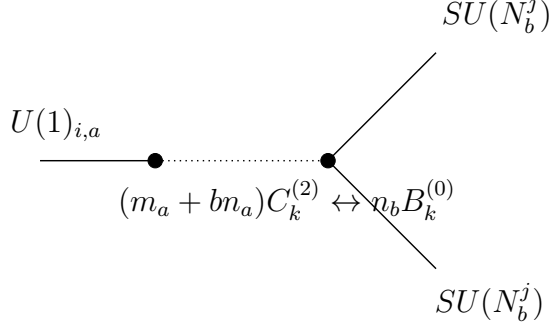


Figure 2: Green-Schwarz counter terms

## 4 NSNS tadpoles

Apart from the RR tadpoles considered in section 2.2, non-supersymmetric theories generically involve also NSNS tadpoles. In this section, we will follow the discussion of [22] in computing the NSNS tadpoles and deriving the effective scalar potential for the closed string moduli. The analysis will be performed at next to leading order in string perturbation theory, i.e. at open string tree level  $e^{-\phi}$ .

The massless NSNS sector fields of our model are the four-dimensional dilaton as well as the internal metric and NSNS two form flux moduli. In our factorized ansatz on  $T^2 \times T^4/\mathbb{Z}_3$ , the moduli of  $T_1$  are the two radions  $R_1$  and  $R_2$  and the two form flux  $b$ . In addition,  $K3$  has 80 moduli. In the orbifold limit  $T^4/\mathbb{Z}_3$ , these moduli are provided for by 11 hyper- and nine tensormultiplets where each of the nine orbifold fixed points contributes one hyper- and one tensormultiplet. The remaining two hypermultiplets originate from the untwisted closed string sector [7]. The twisted NSNS moduli at each fixed point group into a triplet state associated to the complex structure and Kähler deformations of the manifold and a singlet state which originates from the Kaluza Klein reduction of the ten dimensional  $\Omega$  odd form  $B^{(2)}$  on  $\Sigma_k$ . The NSNS triplet and the RR scalar provide the bosonic degrees of freedom of a hypermultiplet, and the NSNS scalar together with the RR two form belong to a tensormultiplet at each orbifold fixed point [31].

The computation of NSNS tadpoles is completely analogous to the one of the RR tadpoles: The tadpoles are extracted from the infrared divergences in the tree channel Klein bottle, annulus and Möbius strip amplitude. These three contributions lead to a sum of perfect squares which can be identified with the disc tadpoles of the various NSNS moduli of the theory. In the  $\Omega\mathcal{R}_1$  orientifold model on  $T^2 \times T^4/\mathbb{Z}_3$ , three contributions to the tadpoles arise at next to leading order. Two of them, the dilaton tadpole and the tadpole of the complex structure on  $T_1$ , originate from the untwisted part of the amplitudes. They have the interpretation given in [22] which we will shortly

repeat here. Additionally, a third tadpole is generated by the twisted moduli corresponding the fixed points of  $T^4/\mathbb{Z}_3$ .

In detail, for the dilaton tadpole we obtain

$$\langle\phi\rangle_D = \frac{1}{\sqrt{\text{Vol}(T^6)}} \left( \sum_{a=1}^K N_a \text{Vol}(\text{D8}_a) - 16\text{Vol}(\text{O8}_a) \right) \quad (45)$$

with

$$\begin{aligned} \text{Vol}(\text{D8}_a) &= \omega L_a = \omega \sqrt{(n_a R_1)^2 + ((m_a + b n_a) R_2)^2}, \\ \text{Vol}(\text{O8}_a) &= \omega R_1, \end{aligned}$$

and the tadpole for the imaginary part of the complex structure on  $T_1$  is given by

$$\langle u \rangle_D = \frac{1}{\sqrt{\text{Vol}(T^6)}} \left( \sum_{a=1}^K N_a \frac{(n_a R_1)^2 - ((m_a + b n_a) R_2)}{L_a} - 16\text{Vol}(\text{O8}_a) \right). \quad (46)$$

As explained in [22], the dilaton tadpole gives the effective tension of the brane configuration in four dimensions. In contrast to the type IIB models constructed in [25, 26], the real part of the complex structure in the T-dual picture with background fields, i.e. the antisymmetric NSNS two form, is not a modulus of the orientifold theory, and therefore we only obtain a tadpole for the imaginary part. Defining  $u = \sqrt{|U_2|} = \sqrt{R_1/R_2}$ , the dilaton and the complex structure tadpole can be cast in the form

$$\langle\phi\rangle_D = \sqrt{\omega} \left( \sum_{a=1}^K N_a \mathcal{L}_a - 16u \right) \quad (47)$$

$$\langle u \rangle_D = u \frac{\partial}{\partial u} \left( \sqrt{\omega} \left( \sum_{a=1}^K N_a \mathcal{L}_a - 16u \right) \right) \quad (48)$$

with

$$\mathcal{L}_a(U) = \sqrt{(n_a u)^2 + ((m_a + U_1 n_a) \frac{1}{u})^2}.$$

The formulas (47) and (48) reflect the fact that, regarding  $T_1$  where the reflexion  $\mathcal{R}_1$  acts, only the left-right symmetric states of the closed string Hilbert space, in this case the complex structure modulus, couple to the crosscaps and boundary states whereas the left-right antisymmetric ones, here the Kähler modulus, do not. In addition, we expect to find couplings to the moduli of  $K3$ . Indeed, a third tadpole arises from the twisted sector which can be cast into the form

$$\langle\varphi_k\rangle_D = \left( \sum_a \text{tr}(\gamma_a) \mathcal{L}_a - 4u \right). \quad (49)$$

From

$$\langle\phi\rangle_D \sim \frac{\partial V}{\partial \phi} \quad \langle u \rangle_D \sim \frac{\partial V}{\partial u} \quad \langle\varphi_k\rangle_D \sim \frac{\partial V}{\partial \varphi_k} \quad (50)$$

we can derive an ansatz for the scalar potential in the string frame of the form

$$V(\phi, U, \varphi_k) = e^{-\phi} \left( \sum_{a=1}^K N_a \mathcal{L}_a - 16u + \varphi_k \left( \sum_{a=1}^K \text{tr}(\gamma_a) \mathcal{L}_a - 4u \right) \right). \quad (51)$$

This potential is only leading order in string theory although higher powers of the complex structure modulus occur. The ansatz (51) for the scalar potential can be compared with the field theory expectation obtained from the Dirac-Born-Infeld action of a  $D9_a$  brane with constant magnetic and electric background flux in the T-dual picture in the limit  $\varphi_k \rightarrow 0$ ,

$$S_{BI} = -T_9 \int_{D9_a} d^{10}x e^{-\phi} \sqrt{\det(G + \mathcal{F}_a)} \quad (52)$$

with the D9-brane tension  $T_9 = \frac{\sqrt{\pi}}{16\kappa_0} 4\pi^2 \alpha'$  and the constant values on  $T_1$

$$G = \mathbb{I}_2, \quad \mathcal{F}_a^{45} = (B + F)_a^{45} = \frac{(m_a + bn_a)\alpha'}{n_a R_1 R_2}. \quad (53)$$

In addition, to lowest order in the  $K3$  moduli the relation

$$\det G(K3) = \text{vol}(K3) = \omega \quad (54)$$

is valid. The dependence on the blow-up modes  $\varphi_k$  in the orbifold limit  $T^4/\mathbb{Z}_3$  seems to be much more complicated and will not be further pursued here.

The scalar potential (51) computed from string theory is unstable to lowest order. This means that the minimum of the theory is not chosen in an appropriate way and hints to an instability of the brane configuration. In the T-dual theory, the tilting of branes towards the  $x^4$  axis corresponds to the dynamical decompactification to the six-dimensional supersymmetric theory. As mentioned in section 2.3, it seems to be impossible to obtain a consistent chiral theory which does not contain any tachyon at all. The problem of stability in the context of tachyons in a purely toroidal compactification has also been addressed in [21].

## 5 Examples

In this section we discuss four models in view of their phenomenological relevance. The tadpole conditions (32), (33) severely restrict the possible choices of gauge groups. For example, the GUT gauge group  $SU(5)$  can only be obtained from  $N_a^0 = 5$  if we restrict our attention to branes (i.e. we do not want to include anti-branes) and we would have to introduce at least to more stacks of branes leading to exotic matter. Furthermore, the generic spectrum in table 1 shows that only an even number of antisymmetric representations of  $SU(N_a^0 = 5)$  can be engineered. Therefore, we will not further pursue GUT models, but show two models which include the gauge group  $SU(3) \times SU(2) \times U(1)_Y$  and two left-right symmetric models which contain  $SU(3) \times SU(2)_L \times SU(2)_R \times U(1)_{B-L}$ . In order to obtain a phenomenologically appealing spectrum, we also include parallelly displaced branes and anti-branes. In all four models we choose the non-trivial background  $b = 1/2$  as only in this case an odd number of generations is achievable.

### 5.1 Example 1a: $SU(3) \times SU(2) \times U(1)^3$ and four generations

In the first example, we choose three different stacks of branes,

$$\begin{aligned} N_A^1 &= 3, & (n_A, m_A) &= (2, -1), \\ N_B^0 &= 2, & (n_B, m_B) &= (4, -1), \\ N_C^1 &= 1, & (n_C, m_C) &= (1, 0). \end{aligned} \quad (55)$$

The brane configuration is depicted in figure 3. This model has already been presented in [28]. The

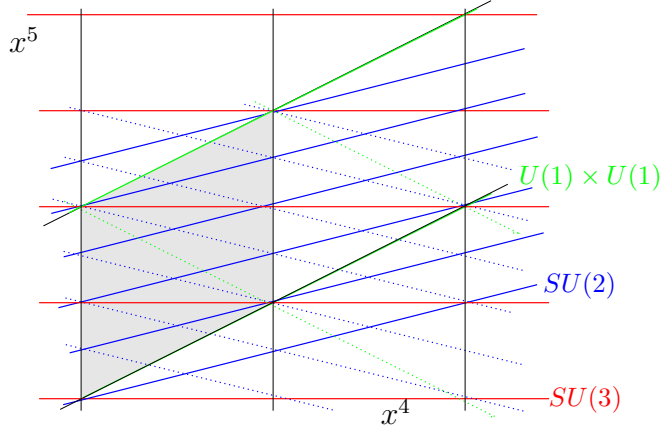


Figure 3: Example 1a: Brane Configuration on  $T_1$ . The shaded area emphasises the fundamental cell of the torus. Solid lines denote D-branes, dotted lines denote their mirror images.

stack of branes of type  $A$  is  $\Omega\mathcal{R}_1$  invariant. Thus, the modified tadpole conditions (32), (33) hold and the spectrum can be read off from tables 1 and 2. In this attempt, we only include branes and require that quarks have no tachyonic partners. In addition, we want to avoid exotic matter which would arise from additional stacks of branes with non-abelian gauge groups. This fixes the numbers  $N_A^1$  and  $N_B^0$  as well as the corresponding wrapping numbers  $n_A, n_B$  along the  $\mathcal{R}_1$  invariant direction. It also fixes the number of quark generations to be even. The spectrum obtained from the setting (55) is displayed in table 3 where we have also listed the original ( $Q_a^i$ ) and anomaly-free ( $Q_Y, \tilde{Q}$ )  $U(1)$  charges. The factor  $U(1)_{1,A}$  which arises from the  $\Omega\mathcal{R}_1$  stack of branes is anomaly-free by itself. In addition, there are two more anomaly-free linear combinations,

$$\begin{aligned} Q_Y &= \frac{Q_A^1}{3} + Q_C^1 - Q_C^2, \\ \tilde{Q} &= \frac{Q_B^0}{4} + Q_C^1 + Q_C^2, \end{aligned} \quad (56)$$

where  $Q_Y$  can be interpreted as hypercharge for the left- and right-handed quarks and leptons. The remaining anomalous  $U(1)$  factor acquires a mass by the generalized Green-Schwarz mechanism as described in section 3 and decouples from the effective theory. In the  $AC\alpha^0, BB'\alpha^0$  and  $CC'\alpha^0$  sectors, tachyonic pseudo-superpartners occur, whereas all other sectors have either massless or massive scalar partners transforming in the same representation.

## 5.2 Example 1b: $SU(3) \times SU(2) \times U(1)^2$ and four generations

The chiral fermion content of example 1a discussed in section 5.1 contains a different number of particles and anti-particles, namely four candidates for quarks and six candidates for anti-quarks, and also a different amount of quarks and leptons. Bearing in mind the considerations made in engineering model 1a, we modify the third type of brane  $C$  such that the amount of quarks and leptons matches. This can be achieved by

$$\begin{aligned} N_A^1 &= 3, & (n_A, m_A) &= (2, -1), \\ N_B^0 &= 2, & (n_B, m_B) &= (4, -1), \\ N_C^1 &= 1, & (n_C, m_C) &= (2, -1), \end{aligned} \quad (57)$$

where the stacks  $C$  and  $A$  are parallelly displaced. The distance of the branes serves to break  $SU(4)$  down to  $SU(3) \times U(1)$ . In the T-dual picture, distances translate into Wilson lines. The brane

Chiral fermionic spectrum for example 1a								
	mult.	rep. of $SU(3) \times SU(2)$	$Q_C^1$	$Q_C^2$	$Q_B^0$	$Q_A^1$	$Q_Y$	$\tilde{Q}$
$AB\alpha^1$	2	$(\bar{3}, 2)$	0	0	-1	-1	-1/3	-1/4
$\alpha^2$	2	$(3, 2)$	0	0	-1	1	1/3	-1/4
$AC\alpha^0$	2	$(\bar{3}, 1)$	1	0	0	-1	2/3	1
	2	$(3, 1)$	0	1	0	1	-2/3	1
$\alpha^1$	1	$(3, 1)$	0	-1	0	1	4/3	-1
$\alpha^2$	1	$(\bar{3}, 1)$	-1	0	0	-1	-4/3	-1
$BC\alpha^1$	1	$(1, 2)$	-1	0	1	0	-1	-3/4
$\alpha^2$	1	$(1, 2)$	0	-1	1	0	1	-3/4
$BC'\alpha^1$	3	$(1, 2)$	-1	0	-1	0	-1	-5/4
$\alpha^2$	3	$(1, 2)$	0	-1	-1	0	1	-5/4
$BB'\alpha^0$	4	$(1, 1_a)$	0	0	2	0	0	1/2
	6	$(1, 1_a) + (1, 3_s)$	0	0	2	0	0	1/2
$CC'\alpha^0$	2	$(1, 1)$	1	1	0	0	0	2

Table 3: Chiral fermionic spectrum for example 1a

configuration is displayed in figure 4. As one can easily see from this figure, locating the stack  $C$  at  $x^5 = R_2/4$  and taking into account lattice shifts gives again an  $\Omega\mathcal{R}_1$  configuration.<sup>1</sup> In this case, we obtain four generations of quarks and leptons as well as several exotic fermions. The complete spectrum is listed in table 4. In this case,  $Q_B^0$  becomes massive while  $Q_A^1$  and  $Q_C^1$  are anomaly-free by themselves. The linear combination  $Q_Y = \frac{Q_A^1}{3} + Q_C^1$  can be interpreted as the SM hypercharge.

### 5.3 Example 2a: $SU(3) \times SU(2)_L \times SU(2)_R \times SO(8) \times U(1)^3$ and three generations

So far, we have only managed to engineer an even number of generations of the SM gauge group even though we have switched on a non-trivial background field  $b$ . The following examples are chosen to be left-right symmetric and contain three generations of left-handed quarks and leptons. We again choose the  $SU(3)$  factor to arise from the  $\Omega\mathcal{R}_1$  invariant position and the  $SU(2)_L \times SU(2)_R$  factors to be supported by branes at non-trivial angles. In order to fulfill the tadpole conditions (32), (33), an additional gauge group  $SO(8)$  as well as an anti-brane have to be included. The brane

<sup>1</sup>Locating a brane  $c$  at  $x^5 = R_2/4$  is convenient, but not necessary. For  $m_c + bn_c = 0$ , equation (27) does not give any constraint on the  $\gamma$  matrices. The second choice consistent with the closure of the orbifold group is  $\gamma_{\Omega\mathcal{R}_1}^c = \gamma_{\Omega\mathcal{R}_1}^{c'} = \mathbb{I}_{N_c}$  and  $\gamma_{\Theta}^c = \gamma_{\Theta}^{-1, c'} = \text{diag}(\mathbb{I}_{N_c^0}, e_{N_c^1}^{2\pi i/3}, e_{N_c^2}^{-2\pi i/3})$  for  $c \neq c'$ . In this case,  $N_c^1$  and  $N_c^2$  can be chosen independently.

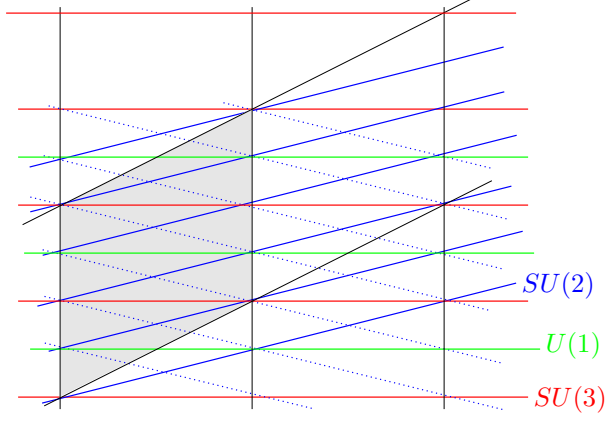


Figure 4: Example 1b: Brane Configuration on  $T_1$

Chiral fermionic spectrum for example 1b					
	mult.	rep. of $SU(3) \times SU(2)$	$Q_B^0$	$Q_A^1$	$Q_C^1$
$AB\alpha^1$	2	$(\bar{3}, 2)$	-1	-1	0
$\alpha^2$	2	$(3, 2)$	-1	1	0
$BC\alpha^1$	2	$(1, 2)$	-1	0	-1
$\alpha^2$	2	$(1, 2)$	-1	0	1
$BB'\alpha^0$	10	$(1, 1_a)$	2	0	0
	6	$(1, 3_s)$	2	0	0

Table 4: Chiral fermionic spectrum for example 1b

configuration of our first choice

$$\begin{aligned}
 & \left. \begin{aligned} N_A^0 &= 8 \\ N_A^1 &= 3 \end{aligned} \right\} & (n_A, m_A) &= (2, -1), \\
 & N_B^1 = 2, & (n_B, m_B) &= (1, 0), \\
 & N_C^1 = 1, & (n_C, m_C) &= (-1, 0),
 \end{aligned} \tag{58}$$

with a parallel displacement of the branes  $B$  and anti-brane  $C$  is shown in figure 5. The complete spectrum is listed in table 5 of appendix D. It contains three generations of quarks and leptons as well as their anti-particles. In addition, it contains exotic matter transforming in the fundamental representation of  $SO(8)$ , a  $(2, 2)$  of  $SU(2)_L \times SU(2)_R$  whose tachyonic partner could be interpreted as a non-standard Higgs particle and several singlets of the non-abelian gauge groups. The anomaly-



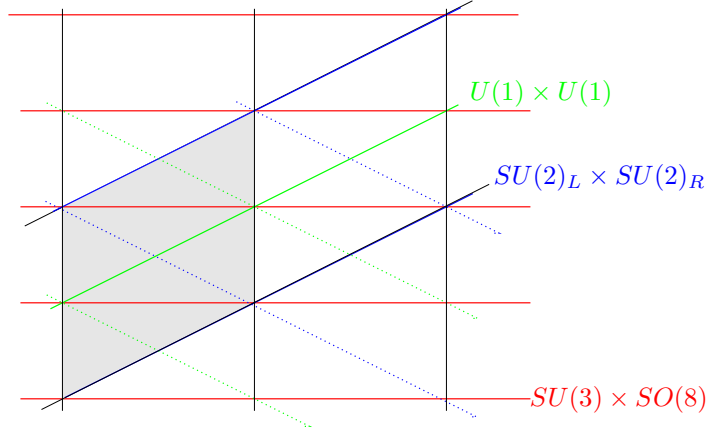


Figure 5: Example 2a: Brane Configuration on  $T_1$

free  $U(1)$ s are given by

$$\begin{aligned}
Q_{B-L} &= -\frac{1}{3}Q_A^1 + Q_C^1 - Q_C^2, \\
Q' &= -\frac{2}{3}Q_A^1 + Q_B^1 - Q_B^2, \\
Q'' &= \frac{1}{4}(Q_B^1 + Q_B^2 + 2Q_C^1 + 2Q_C^2),
\end{aligned} \tag{59}$$

where  $Q_{B-L}$  can be interpreted as Baryon - Lepton number occurring in left-right symmetric models.

There are two facts which have to be taken care of when including anti-branes. On the one hand, the GSO-projection in the brane - anti-brane sector is opposite to the usual one and results in selecting the reverse chirality. On the other hand, the  $\Omega\mathcal{R}_1$  projection in the  $CC'$  sector selects the symmetric instead of the antisymmetric representation in the R sector. Due to the displacement of the stacks  $B$  and  $C$ , there will be no tachyons stretched between parallel branes and anti-branes as long as  $R_1$  and  $R_2$  are chosen big enough.

In this example, tachyonic pseudo-superpartners  $\psi_{\Delta\varphi-1/2}^1|0\rangle_{NSNS}$  occur in the  $AB\alpha^0$ ,  $BB'\alpha^0$  and  $CC'\alpha^0$  sectors. In the  $AC\alpha^0$  and  $BC'\alpha^0$  sectors, the reversed GSO-projection leaves the tachyonic groundstate  $|0\rangle_{NSNS}$  invariant.

#### 5.4 Example 2b: $SU(3) \times SU(2)_L \times SU(2)_R \times SO(8) \times U(1)^2$ and three generations

As a last example, we start with the same  $SU(3) \times SU(2)_L \times SU(2)_R$  configuration as in example 2a, but choose the anti-brane  $C$  to be  $\Omega\mathcal{R}_1$  invariant and parallelly displaced w.r.t. the  $SU(3)$  stack. The brane positions resulting from

$$\begin{aligned}
\left. \begin{aligned} N_A^0 &= 8 \\ N_A^1 &= 3 \end{aligned} \right\} & (n_A, m_A) = (2, -1), \\
N_B^1 &= 2, & (n_B, m_B) = (1, 0), \\
N_C^1 &= 1, & (n_C, m_C) = (-2, 1)
\end{aligned} \tag{60}$$

are displayed in figure 6. The complete chiral spectrum is listed in table 6 of appendix D, and the

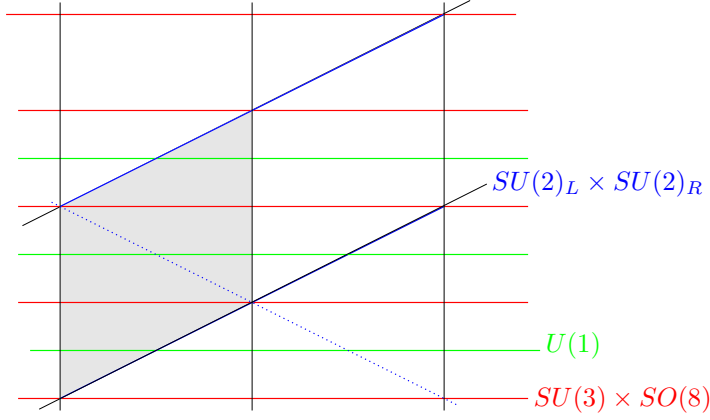


Figure 6: Example 2b: Brane Configuration on  $T_1$

anomaly free  $U(1)$  factors are given by

$$\begin{aligned} Q_{B-L} &= -\frac{1}{3}Q_A^1 - Q_C^1, \\ Q' &= Q_B^1 - Q_B^2 + 2Q_C^1. \end{aligned} \quad (61)$$

In this case, the spectrum contains three generations of left- and right-handed quarks and leptons beside some exotic matter, the GSO-projection is reversed in the  $AC$  and  $BC$  sectors, and tachyons with the same representation of the gauge group as the fermions appear in the  $AB\alpha^0$ ,  $BB'\alpha^0$  and  $BC\alpha^0$  sectors.

## 6 Discussion and Conclusions

In this paper, we have derived the tadpole conditions and chiral spectra of type IIA orientifolds on  $T^2 \times T^4/\mathbb{Z}_3$  with D8-branes at non-trivial angles on  $T^2$ . This class of models is T-dual to  $\Omega\mathcal{R}_1I_4$  orientifolds with the same orbifold group  $\mathbb{Z}_3$  (where  $I_4$  is the reflexion of all four coordinates of the orbifold) but D4-branes instead of D8-branes. The dual D4-branes are transverse to the four dimensional orbifold. As the Planck scale in these models obtained from dimensional reduction depends on the volume  $\omega$  of the orbifold,

$$M_P \sim \frac{\sqrt{R_1 R_2 \omega}}{\lambda_s \alpha'^2}, \quad (62)$$

choosing  $\omega$  large can lower the string scale down to the TeV range. In the same T-dual picture, the gauge couplings arising from  $D4_a$  branes are at tree level given by [26]

$$\frac{2\pi}{g_a^2} = \frac{M_s}{\lambda_s} L_a. \quad (63)$$

Applying this relationship to the examples discussed in the previous section, we obtain

$\frac{\alpha_{QCD}}{\alpha_2} = 2\sqrt{1 + \frac{1}{16}\frac{1}{u^4}}$  for examples 1a and 1b and  $\frac{\alpha_{QCD}}{\alpha_2} = \frac{1}{2}\sqrt{1 + \frac{1}{4}\frac{1}{u^4}}$  for examples 2a and 2b, where  $u = \sqrt{R_1/R_2}$  is as defined in section 4. These values are only valid at tree level at the string scale  $M_s$ . In order to make contact with the observed data at the electroweak scale, the running of couplings as well as loop corrections which might be large would have to be taken into account.

The qualitative behaviour of Yukawa couplings (8) can be nicely read off from figure 3 for example 1a. The sizes  $A_{ijk}$  of the smallest triangular worldsheets in units of  $\frac{R_1 R_2}{\alpha'}$  are  $\frac{1}{48}, \frac{1}{16}, \frac{1}{12}$

and  $\frac{1}{4}$ . There exist, however, also trilinear couplings which arise from one single intersection point. The reason for this is that in example 1a, two quark generations  $Q_L^{1,2}$  are realised as  $(\bar{3}, 2)$  and the other two  $Q_L^{3,4}$  as  $(3, 2)$  in the  $AB$  sector. Couplings with higgs scalars  $h$  from the  $BB'$  sector are allowed by regarding the quantum numbers. Since the position of branes  $A$  is chosen to be  $\Omega\mathcal{R}_1$  invariant, the intersection points of  $AB$  are also intersection points of  $BB'$ .

Let us now briefly comment on example 2b. In this case, all left handed quarks  $Q_L^i$  are realised as  $(\bar{3}, 2_L)$  while all right handed quarks  $Q_R^j$  transform as  $(3, 2_R)$ . All quarks arise from the  $AB$  sector where  $A$  is the  $\Omega\mathcal{R}_1$  invariant stack of branes. The  $BB'$  sector can provide for higgs scalars  $h$  in the  $(2_L, 2_R)$  with  $U(1)$  charges  $Q_B^1 = Q_B^2 = \pm 1$ . The quantum numbers thus allow for trilinear couplings of the form  $hQ_L^i Q_R^j$  (for  $i, j = 1, 2$  and  $i = j = 3$  since the third generation differs in the quantum numbers  $Q_B^1, Q_B^2$  from the other two). In the same spirit, trilinear couplings  $hL_L^i L_R^j$  of a higgs particle with two leptons  $L_L^i, L_R^j$  are allowed for  $i, j = 1, 2$  and  $i = j = 3$ . But in contrast to the couplings involving quarks, the leptons arise from the  $BC$  sector which does not have any common intersection point with the  $BB'$  sector. Naively, one can therefore speculate that quark and lepton masses are generated from couplings to the same higgs scalars  $h$  acquiring a vev, and that there will be a hierarchy of quark and lepton masses since the relevant worldsheets are of the order  $A_{hQQ} = 0$  and  $A_{hLL} \sim \mathcal{O}(\frac{R_1 R_2}{\alpha'})$ . This naive interpretation, however, has to be handled with care since not all types of couplings to higgses might occur (e.g. if only one type of scalar particles  $h$  with  $Q_B^1 = Q_B^2 = 1$  exists and no couplings  $\bar{h}QQ$  are allowed).

In summary, we have computed the tadpole cancellation conditions and generic spectra for orientifold models with intersecting D8-branes which have a T-dual description in terms of D4-branes at angles. The conditions (32), (33) severely restrict the achievable gauge groups. We have given two examples with the SM gauge group and two further left-right symmetric examples, in which a tachyon that necessarily arises from intersecting mirror branes might play the role of a non-standard Higgs particle. In addition, we have computed the NSNS tadpoles in next to leading order. In this approximation, the scalar potential depends linearly on the twisted moduli of the orbifold, and it would be interesting to examine in more detail if they can contribute in stabilizing the non-supersymmetric models with branes at angles.

Another ansatz for improved models is to consider more complicated orbifold groups which could project out the tachyons completely.

## Acknowledgments

It is a pleasure to thank Stefan Förste and Ralph Schreyer for discussions. Furthermore, I acknowledge discussions with Ralph Blumenhagen and Boris Körs.

This work is supported by the European Commission RTN programs HPRN-CT-2000-00131, 00148 and 00152.

## A Computation of 1-loop diagrams

### A.1 Lattice contributions on $(T^4/Z_3)/\Omega\mathcal{R}_1$

The general form of the lattice sums on  $T^4/Z_3$  for one  $T^2$  in the loop-channel is given by ( $\rho \equiv R^2/\alpha'$ )

$$\mathcal{L}^R[\alpha](t) \equiv \sum_{m,n \in \mathbb{Z}} e^{-\alpha\pi t(m^2 + mn + n^2)/\rho}. \quad (64)$$

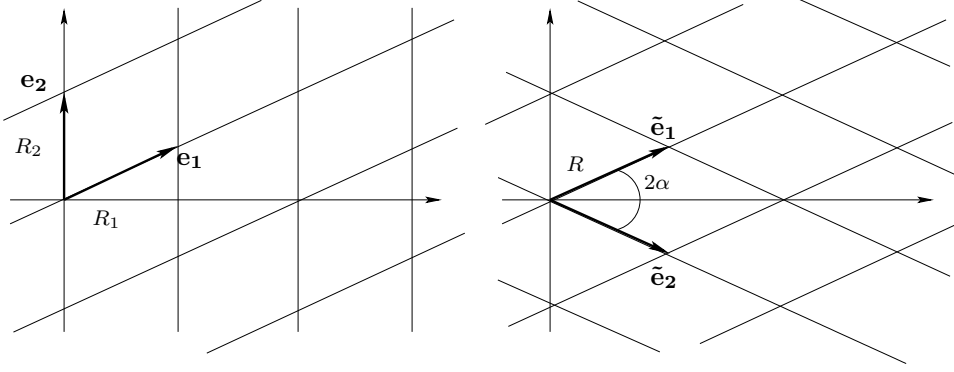


Figure 7: Two ways to parameterize the lattice with  $b = 1/2$

Using the Poisson resummation formula

$$\sum_{x \in \Gamma} = \frac{1}{\text{vol}(\Gamma)} \sum_{p \in \Gamma^*} \tilde{f}(p) \quad (65)$$

for a  $d$ -dimensional lattice  $\Gamma$  and its dual lattice  $\Gamma^*$  with the Fourier transform  $\tilde{f}(p) = \int_{\mathbb{R}^d} dx e^{2\pi i x \cdot p} f(x)$  and defining  $t = 1/\kappa l$  gives the lattice sums in the tree-channel

$$\mathcal{L}^R[\alpha](t) = l \frac{2\kappa}{\sqrt{3}\alpha} \rho \mathcal{L}^{1/R} \left[ \frac{4\kappa}{3\alpha} \right] (l). \quad (66)$$

For  $T^4/Z_3$ , we thus obtain

$$\text{Klein bottle:} \quad (\mathcal{L}^{R_1} \mathcal{L}^{R_2}) [1](t) = \frac{64}{3} l^2 \omega \left( \mathcal{L}^{1/R_1} \mathcal{L}^{1/R_2} \right) [16/3](l) \quad (67)$$

$$\text{Annulus:} \quad (\mathcal{L}^{R_1} \mathcal{L}^{R_2}) [2](t) = \frac{4}{3} l^2 \omega \left( \mathcal{L}^{1/R_1} \mathcal{L}^{1/R_2} \right) [4/3](l) \quad (68)$$

$$\text{Möbius strip:} \quad (\mathcal{L}^{R_1} \mathcal{L}^{R_2}) [2](t) = \frac{64}{3} l^2 \omega \left( \mathcal{L}^{1/R_1} \mathcal{L}^{1/R_2} \right) [16/3](l) \quad (69)$$

where  $\omega \equiv \rho_1 \rho_2$  is the volume of the orbifold in units of  $\alpha'$ .

## A.2 Lattice contributions on $T^2/\Omega\mathcal{R}_1$

The lattice contributions of  $T^2$  where the reflexion  $\mathcal{R}_1$  acts are as given in [23]. The result for the **b** type lattice can be recast in the notation of [19] with non-vanishing background  $b = 1/2$  field in the T-dual picture by replacing

$$\begin{aligned} \tan \alpha &= \frac{R_2}{2R_1}, \\ R^2 &= R_1^2 + (R_2/2)^2, \\ \tilde{\mathbf{e}}_1 &= \mathbf{e}_1, \\ \tilde{\mathbf{e}}_2 &= \mathbf{e}_1 - \mathbf{e}_2, \\ (\tilde{n}, \tilde{m}) &= (n + m, -m), \end{aligned} \quad (70)$$

where the definitions are given in figure 7.

### A.3 Intersection numbers and angles on the deformed $T^2$

Multiplicities of chiral fermions are given in terms of the intersection numbers where  $b = 0, 1/2$  are the two possible choices of background field in the T-dual picture,

$$\begin{aligned}
I_{ab} &= n_a m_b - n_b m_a, \\
I_{aa'} &= -(2m_a n_a + (2b)n_a^2), \\
I_{aa'}^{\Omega\mathcal{R}_1} &= -(2m_a + (2b)n_a), \\
I_{aa'} - I_{aa'}^{\Omega\mathcal{R}_1} &= -(2m_a + (2b)n_a)(n_a - 1).
\end{aligned} \tag{71}$$

The angles contained in the open string 1-loop amplitudes can be re-expressed in terms of the wrapping numbers,

$$\begin{aligned}
\frac{1}{\tan(\pi\varphi)} &= \frac{n_a}{(m_a + bn_a)} \frac{R_1}{R_2}, \\
\frac{1}{\tan(\pi\Delta\varphi_{ab})} &= -\frac{1}{I_{ab}} n_a n_b \frac{R_1}{R_2} - \frac{1}{I_{ab}} (m_a + bn_a)(m_b + bn_b) \frac{R_2}{R_1}, \\
\frac{I_{aa'}^{\Omega\mathcal{R}_1}}{\tan(\pi\varphi)} &= -2n_a \frac{R_1}{R_2}.
\end{aligned} \tag{72}$$

### A.4 Oscillator contributions

Oscillator contributions to the 1-loop amplitudes can be expressed in terms of generalized  $\vartheta$  functions. The relevant formulas for untwisted sectors without insertions can be found e.g. in [10]. In addition, an insertion of  $\Theta^k$  in the trace leads to

$$\text{Klein bottle: } \mathcal{K}^{(k)} = \frac{\vartheta \begin{bmatrix} 0 \\ 1/2 \end{bmatrix}^2}{\eta^6} \prod_{i=2,3} \frac{\vartheta \begin{bmatrix} 0 \\ 1/2+2kv_i \end{bmatrix}}{\vartheta \begin{bmatrix} 1/2 \\ 1/2+2kv_i \end{bmatrix}} (2t), \tag{73}$$

$$\text{Annulus: } \mathcal{A}_{ab}^{(k)} = i \frac{\vartheta \begin{bmatrix} 0 \\ 1/2 \end{bmatrix}}{\eta^3} \frac{\vartheta \begin{bmatrix} \Delta\varphi \\ 1/2 \end{bmatrix}}{\vartheta \begin{bmatrix} 1/2+\Delta\varphi \\ 1/2 \end{bmatrix}} \prod_{i=2,3} \frac{\vartheta \begin{bmatrix} 0 \\ 1/2+kv_i \end{bmatrix}}{\vartheta \begin{bmatrix} 1/2 \\ 1/2+kv_i \end{bmatrix}} (t), \tag{74}$$

$$\text{Möbius strip: } \mathcal{M}_a^{(k)} = ie^{2\pi i\varphi} \frac{\vartheta \begin{bmatrix} 1/2 \\ 0 \end{bmatrix}}{\eta^3} \frac{\vartheta \begin{bmatrix} 1/2+2\varphi \\ -\varphi \end{bmatrix}}{\vartheta \begin{bmatrix} 1/2+2\varphi \\ 1/2-\varphi \end{bmatrix}} \prod_{i=2,3} \frac{\vartheta \begin{bmatrix} 1/2 \\ kv_i \end{bmatrix}}{\vartheta \begin{bmatrix} 1/2 \\ 1/2+kv_i \end{bmatrix}} (t + \frac{i}{2}). \tag{75}$$

By modular transformation to the tree-channel, one obtains contributions from oscillators in the  $k^{\text{th}}$  twisted sector,

$$\text{Klein bottle: } \tilde{\mathcal{K}}^{(k)} = \frac{\vartheta \begin{bmatrix} 1/2 \\ 0 \end{bmatrix}^2}{\eta^6} \prod_{i=2,3} \frac{\vartheta \begin{bmatrix} 1/2-2kv_i \\ 0 \end{bmatrix}}{\vartheta \begin{bmatrix} 1/2-2kv_i \\ 1/2 \end{bmatrix}} (2l), \quad (76)$$

$$\text{Annulus: } \tilde{\mathcal{A}}_{ab}^{(k)} = \frac{\vartheta \begin{bmatrix} 1/2 \\ 0 \end{bmatrix}}{\eta^3} \frac{\vartheta \begin{bmatrix} 1/2 \\ \Delta\varphi \end{bmatrix}}{\vartheta \begin{bmatrix} 1/2 \\ 1/2+\Delta\varphi \end{bmatrix}} \prod_{i=2,3} \frac{\vartheta \begin{bmatrix} 1/2-kv_i \\ 0 \end{bmatrix}}{\vartheta \begin{bmatrix} 1/2-kv_i \\ 1/2 \end{bmatrix}} (2l), \quad (77)$$

$$\text{Möbius strip: } \tilde{\mathcal{M}}_a^{(k)} = \frac{\vartheta \begin{bmatrix} 1/2 \\ 0 \end{bmatrix}}{\eta^3} \frac{\vartheta \begin{bmatrix} 1/2 \\ \varphi \end{bmatrix}}{\vartheta \begin{bmatrix} 1/2 \\ 1/2+\varphi \end{bmatrix}} (2l + \frac{i}{2}) \prod_{i=2,3} \frac{\vartheta \begin{bmatrix} -kv_i \\ 1/2 \end{bmatrix} \vartheta \begin{bmatrix} 1/2-kv_i \\ 0 \end{bmatrix}}{\vartheta \begin{bmatrix} 1/2-kv_i \\ 1/2 \end{bmatrix} \vartheta \begin{bmatrix} -kv_i \\ 0 \end{bmatrix}} (4l). \quad (78)$$

## B Tree channel results for $(T^2 \times T^4/Z_3)/\Omega\mathcal{R}_1$

### B.1 Crosscap states

The crosscap conditions for the  $\Omega\mathcal{R}_1$ -model are

$$\left[ X_{L,R}^i(\sigma, 0) - \Theta^k X_{R,L}^i(\sigma + \pi, 0) \right] |\Omega\mathcal{R}_1\Theta^k\rangle = 0, \quad (79)$$

$$\left[ X_{L,R}^{\bar{i}}(\sigma, 0) - \Theta^k X_{R,L}^{\bar{i}}(\sigma + \pi, 0) \right] |\Omega\mathcal{R}_1\Theta^k\rangle = 0. \quad (80)$$

Inserting the mode expansion

$$X^i(\sigma, \tau) = x^i + \frac{p_L^i}{2\pi}(\tau + \sigma) + \frac{p_R^i}{2\pi}(\tau - \sigma) + \frac{i}{2} \sum_r \frac{1}{r} \alpha_r^i e^{-ir(\tau+\sigma)} + \frac{i}{2} \sum_s \frac{1}{s} \tilde{\alpha}_s^i e^{-is(\tau-\sigma)} \quad (81)$$

gives the following constraints on  $T^4/\mathbb{Z}_N$

$$\left. \begin{aligned} & \begin{bmatrix} p_L^i + e^{2\pi i k v_i} p_R^i \\ p_L^{\bar{i}} + e^{-2\pi i k v_i} p_R^{\bar{i}} \\ p_R^i + e^{2\pi i k v_i} p_L^i \\ p_R^{\bar{i}} + e^{-2\pi i k v_i} p_L^{\bar{i}} \end{bmatrix} \end{aligned} \right\} |\Omega\mathcal{R}_1\Theta^k\rangle = 0, \quad (82)$$

$$\left. \begin{aligned} & \begin{bmatrix} \alpha_r^i + e^{\pi i(2kv_i-r)} \tilde{\alpha}_{-r}^i \\ \alpha_s^{\bar{i}} + e^{\pi i(-2kv_i-s)} \tilde{\alpha}_{-s}^{\bar{i}} \\ \tilde{\alpha}_{-r}^i + e^{\pi i(2kv_i-r)} \alpha_r^i \\ \tilde{\alpha}_{-s}^{\bar{i}} + e^{\pi i(-2kv_i-s)} \alpha_s^{\bar{i}} \end{bmatrix} \end{aligned} \right\} |\Omega\mathcal{R}_1\Theta^k\rangle = 0. \quad (83)$$

The set of equations (82) states that for  $k = 0$  windings along all four directions of the orbifold occur while for  $k \neq 0$ , only Kaluza Klein momenta and windings from the first  $T^2$  contribute as discussed in appendix **B** of [23]. The equations (83) are only mutually consistent if  $r \in \mathbb{Z} + 2kv_i$ ,  $s \in \mathbb{Z} - 2kv_i$ . Using the notation  $n \in \mathbb{Z}$ ,  $r \in \mathbb{Z}(+1/2)$  for the R (NS) sector, the oscillator constraints can be rewritten as

$$\left\{ \begin{aligned} & \left[ \alpha_{n+2kv_i}^i + (-1)^n \tilde{\alpha}_{-n-2kv_i}^i \right] \\ & \left[ \alpha_{n-2kv_i}^{\bar{i}} + (-1)^n \tilde{\alpha}_{-n+2kv_i}^{\bar{i}} \right] \end{aligned} \right\} |\Omega \mathcal{R}_1 \Theta^k\rangle = 0, \quad (84)$$

$$\left\{ \begin{aligned} & \left[ \psi_{r+2kv_i}^i + i\eta e^{-i\pi r} \tilde{\psi}_{-r-2kv_i}^i \right] \\ & \left[ \psi_{r-2kv_i}^{\bar{i}} + i\eta e^{-i\pi r} \tilde{\psi}_{-r+2kv_i}^{\bar{i}} \right] \end{aligned} \right\} |\Omega \mathcal{R}_1 \Theta^k\rangle = 0. \quad (85)$$

A solution to these constraints is provided by

$$\begin{aligned} |\Omega \mathcal{R}_1 \Theta^k, \eta\rangle = & \mathcal{N}_C^{(k)} \exp \left\{ - \sum_n \frac{(-1)^n}{n} \alpha_{-n}^\mu \tilde{\alpha}_{-n}^\mu - \sum_n \frac{(-1)^n}{n} \alpha_{-n}^1 \tilde{\alpha}_{-n}^1 - \sum_n \frac{(-1)^n}{n} \alpha_{-n}^{\bar{1}} \tilde{\alpha}_{-n}^{\bar{1}} \right. \\ & - \sum_{i \in \{2,3\}} \sum_n \frac{(-1)^n}{n} \alpha_{-n+2kv_i}^i \tilde{\alpha}_{-n+2kv_i}^{\bar{i}} - \sum_{i \in \{2,3\}} \sum_n \frac{(-1)^n}{n} \alpha_{-n-2kv_i}^{\bar{i}} \tilde{\alpha}_{-n-2kv_i}^i \\ & - i\eta \sum_r e^{-i\pi r} \psi_{-r}^\mu \tilde{\psi}_{-r}^\mu - i\eta \sum_r e^{-i\pi r} \psi_{-r}^1 \tilde{\psi}_{-r}^1 - i\eta \sum_r e^{-i\pi r} \psi_{-r}^{\bar{1}} \tilde{\psi}_{-r}^{\bar{1}} \\ & \left. - i\eta \sum_{i \in \{2,3\}} \sum_r e^{-i\pi r} \psi_{-r+2kv_i}^i \tilde{\psi}_{-r+2kv_i}^{\bar{i}} - i\eta \sum_{i \in \{2,3\}} \sum_r e^{-i\pi r} \psi_{-r-2kv_i}^{\bar{i}} \tilde{\psi}_{-r-2kv_i}^i \right\} |0, \eta\rangle. \end{aligned}$$

The dependence on the lattice is contained in the groundstate  $|0, \eta\rangle$ .

## B.2 Boundary states

In order to reproduce the amplitudes obtained by modular transformation from the loop channel, a boundary state at angle  $\pi\varphi$  on  $T_1$  w.r.t. the  $x^4$  axis has to be of the form

$$\begin{aligned} |\varphi, \Theta^k; \eta\rangle = & \mathcal{N}_B^{(k)} \exp \left\{ - \sum_n \frac{1}{n} \alpha_{-n}^\mu \tilde{\alpha}_{-n}^\mu - \sum_n \frac{1}{n} e^{2\pi i \varphi} \alpha_{-n}^1 \tilde{\alpha}_{-n}^1 - \sum_n \frac{1}{n} e^{-2\pi i \varphi} \alpha_{-n}^{\bar{1}} \tilde{\alpha}_{-n}^{\bar{1}} \right. \\ & - \sum_{i \in \{2,3\}} \sum_n \frac{1}{n} \alpha_{-n+2kv_i}^i \tilde{\alpha}_{-n+2kv_i}^{\bar{i}} - \sum_{i \in \{2,3\}} \sum_n \frac{1}{n} \alpha_{-n-2kv_i}^{\bar{i}} \tilde{\alpha}_{-n-2kv_i}^i \\ & - i\eta \sum_r \psi_{-r}^\mu \tilde{\psi}_{-r}^\mu - i\eta \sum_r e^{2\pi i \varphi} \psi_{-r}^1 \tilde{\psi}_{-r}^1 - i\eta \sum_r e^{-2\pi i \varphi} \psi_{-r}^{\bar{1}} \tilde{\psi}_{-r}^{\bar{1}} \\ & \left. - i\eta \sum_{i \in \{2,3\}} \sum_r \psi_{-r+2kv_i}^i \tilde{\psi}_{-r+2kv_i}^{\bar{i}} - i\eta \sum_{i \in \{2,3\}} \sum_r \psi_{-r-2kv_i}^{\bar{i}} \tilde{\psi}_{-r-2kv_i}^i \right\} |0, \eta\rangle. \end{aligned}$$

As for the crosscap states, the groundstate  $|0, \eta\rangle$  contains Kaluza-Klein momentum and winding eigenvalues from  $T^2$  and windings from  $T^4/\mathbb{Z}_N$ .

## B.3 Zero modes and GSO invariant states

We present the following discussion for the crosscap states. The GSO projections on boundary states are completely analogous.

### B.3.1 NSNS sector

In the NSNS sectors, the GSO projection on the ground state is determined by requiring tachyonic ground states to be unphysical. Therefore, the GSO-invariant combination is

$$|\Omega\mathcal{R}_1\Theta^k\rangle_{NSNS} = |\Omega\mathcal{R}_1\Theta^k, +\rangle_{NSNS} - |\Omega\mathcal{R}_1\Theta^k, -\rangle_{NSNS} \quad (86)$$

### B.3.2 Untwisted RR sector

Defining ( $i = 2, 3$ )

$$\begin{aligned} \psi_\eta^\mu &= \frac{1}{\sqrt{2}} \left( \psi_0^\mu + i\eta\tilde{\psi}_0^\mu \right), \\ \psi_\eta^1 &= \frac{1}{\sqrt{2}} \left( \psi_0^1 + i\eta\tilde{\psi}_0^1 \right), & \psi_\eta^{\bar{1}} &= \frac{1}{\sqrt{2}} \left( \psi_0^{\bar{1}} + i\eta\tilde{\psi}_0^{\bar{1}} \right), \\ \psi_\eta^i &= \frac{1}{\sqrt{2}} \left( \psi_0^i + i\eta\tilde{\psi}_0^i \right), & \psi_\eta^{\bar{i}} &= \frac{1}{\sqrt{2}} \left( \psi_0^{\bar{i}} + i\eta\tilde{\psi}_0^{\bar{i}} \right), \end{aligned} \quad (87)$$

the non-trivial commutation relations are

$$\begin{aligned} \{\psi_+^\mu, \psi_-^\mu\} &= 1, \\ \{\psi_+^1, \psi_-^{\bar{1}}\} &= \{\psi_-^1, \psi_+^{\bar{1}}\} = 1, \\ \{\psi_+^i, \psi_-^{\bar{i}}\} &= \{\psi_-^i, \psi_+^{\bar{i}}\} = 1. \end{aligned} \quad (88)$$

The crosscap conditions from the zero modes in the RR-sector on the groundstate then read

$$\left. \begin{array}{c} \psi_\eta^\mu \\ \psi_\eta^1 \\ \psi_\eta^{\bar{1}} \\ \psi_\eta^i \\ \psi_\eta^{\bar{i}} \end{array} \right\} |\Omega\mathcal{R}_1, \eta\rangle_{RR}^0 = 0, \quad (89)$$

and the zero mode parts of the GSO projections are given by

$$(-1)^F = \prod_{m=2}^9 \sqrt{2} \psi_0^m \quad (90)$$

$$\begin{aligned} &= \prod_{\mu=2,3} (\psi_+^\mu + \psi_-^\mu) \cdot \frac{1}{2i} \left( \psi_+^1 + \psi_-^1 + \psi_+^{\bar{1}} + \psi_-^{\bar{1}} \right) \left( \psi_+^1 + \psi_-^1 - \psi_+^{\bar{1}} - \psi_-^{\bar{1}} \right) \\ &\quad \prod_{i=2,3} \frac{1}{2i} \left( \psi_+^i + \psi_-^i + \psi_+^{\bar{i}} + \psi_-^{\bar{i}} \right) \left( \psi_+^i + \psi_-^i - \psi_+^{\bar{i}} - \psi_-^{\bar{i}} \right) \end{aligned}$$

$$(-1)^{\tilde{F}} = \prod_{m=2}^9 \sqrt{2} \tilde{\psi}_0^m \quad (91)$$

$$\begin{aligned} &= \prod_{\mu=2,3} \frac{1}{i} (\psi_+^\mu - \psi_-^\mu) \cdot \frac{1}{2i} \left( \psi_+^1 - \psi_-^1 + \psi_+^{\bar{1}} - \psi_-^{\bar{1}} \right) \left( \psi_+^1 - \psi_-^1 - \psi_+^{\bar{1}} + \psi_-^{\bar{1}} \right) \\ &\quad \prod_{i=2,3} \frac{1}{2i} \left( \psi_+^i - \psi_-^i + \psi_+^{\bar{i}} - \psi_-^{\bar{i}} \right) \left( \psi_+^i - \psi_-^i - \psi_+^{\bar{i}} + \psi_-^{\bar{i}} \right). \end{aligned}$$



Defining

$$|\Omega\mathcal{R}_1, -\rangle^0 \equiv \left[ \left( \prod_{\mu=2,3} \psi_-^\mu \right) (\psi_-^1 \psi_-^{\bar{1}}) \left( \prod_{i=2,3} \psi_-^i \psi_-^{\bar{i}} \right) \right] |\Omega\mathcal{R}_1, +\rangle^0, \quad (92)$$

the action of the complete GSO-projector can be rephrased as

$$(-1)^F |\Omega\mathcal{R}_1, +\rangle = -(-1)^{\tilde{F}} |\Omega\mathcal{R}_1, +\rangle = -i |\Omega\mathcal{R}_1, -\rangle, \quad (93)$$

$$(-1)^F |\Omega\mathcal{R}_1, -\rangle = -(-1)^{\tilde{F}} |\Omega\mathcal{R}_1, -\rangle = i |\Omega\mathcal{R}_1, +\rangle, \quad (94)$$

and

$$|\Omega\mathcal{R}_1, +\rangle_{RR} - i |\Omega\mathcal{R}_1, -\rangle_{RR} \quad \text{is invariant w.r.t.} \quad P_{GSO} = \frac{1 + (-1)^F}{2} \frac{1 - (-1)^{\tilde{F}}}{2}. \quad (95)$$

### B.3.3 Twisted RR sectors

For  $k \neq 0$ , the zero mode conditions read

$$\left. \begin{array}{l} \psi_\eta^\mu \\ \psi_\eta^1 \\ \psi_\eta^{\bar{1}} \end{array} \right\} |\Omega\mathcal{R}_1 \Theta^k, \eta\rangle_{RR}^0 = 0. \quad (96)$$

The zero mode parts of the GSO projection operators are now given by

$$(-1)^F = \prod_{m=2}^5 \sqrt{2} \psi_0^m \quad (97)$$

$$= \prod_{\mu=2,3} (\psi_+^\mu + \psi_-^\mu) \cdot \frac{1}{2i} (\psi_+^1 + \psi_-^1 + \psi_+^{\bar{1}} + \psi_-^{\bar{1}}) (\psi_+^1 + \psi_-^1 - \psi_+^{\bar{1}} - \psi_-^{\bar{1}}),$$

$$(-1)^{\tilde{F}} = \prod_{m=2}^5 \sqrt{2} \tilde{\psi}_0^m \quad (98)$$

$$= \prod_{\mu=2,3} \frac{1}{i} (\psi_+^\mu - \psi_-^\mu) \cdot \frac{1}{2i} (\psi_+^1 - \psi_-^1 + \psi_+^{\bar{1}} - \psi_-^{\bar{1}}) (\psi_+^1 - \psi_-^1 - \psi_+^{\bar{1}} + \psi_-^{\bar{1}}).$$

Using

$$|\Omega\mathcal{R}_1 \Theta^k, -\rangle^0 \equiv \left[ \left( \prod_{\mu=2,3} \psi_-^\mu \right) (\psi_-^1 \psi_-^{\bar{1}}) \right] |\Omega\mathcal{R}_1 \Theta^k, +\rangle^0 \quad (99)$$

leads to the action of the zero mode part of the GSO projector on the groundstates

$$(-1)^F |\Omega\mathcal{R}_1 \Theta^k, +\rangle^0 = -(-1)^{\tilde{F}} |\Omega\mathcal{R}_1 \Theta^k, +\rangle^0 = i |\Omega\mathcal{R}_1 \Theta^k, -\rangle^0, \quad (100)$$

$$(-1)^F |\Omega\mathcal{R}_1 \Theta^k, -\rangle^0 = -(-1)^{\tilde{F}} |\Omega\mathcal{R}_1 \Theta^k, -\rangle^0 = -i |\Omega\mathcal{R}_1 \Theta^k, +\rangle^0. \quad (101)$$

These relations carry over to the excited states. Thus,

$$|\Omega\mathcal{R}_1 \Theta^k, +\rangle_{RR} + i |\Omega\mathcal{R}_1 \Theta^k, -\rangle_{RR} \quad \text{is invariant w.r.t.} \quad P_{GSO} = \frac{1 + (-1)^F}{2} \frac{1 - (-1)^{\tilde{F}}}{2}. \quad (102)$$

## C Massless states and chiral fermions for $T^2 \times T^4/\mathbb{Z}_3$

The lightest mass eigenstates are distinguished by their  $\Theta$  eigenvalues. Defining  $\alpha \equiv e^{2\pi i/3}$ , the lightest bosonic and fermionic states between branes  $a$  and  $b$  at angle  $\pi\Delta\varphi$  on  $T^2$  are listed in the following tables.

Bosonic open spectrum of $T^2 \times T^4/\mathbb{Z}_3$			
on $T^2$	state	mass	$\mathbb{Z}_3$
$\Delta\varphi = 0$	$\psi_{-1/2}^\mu 0\rangle$	0	1
	$\psi_{-1/2}^{1,1} 0\rangle$	0	1
	$\psi_{-1/2}^{2,3} 0\rangle$	0	$\alpha$
	$\psi_{-1/2}^{2,3} 0\rangle$	0	$\alpha^2$
$\Delta\varphi \neq 0$	$\psi_{-1/2}^\mu 0\rangle$	$\frac{1}{2}\Delta\varphi$	1
	$\psi_{\Delta\varphi-1/2}^1 0\rangle$	$-\frac{1}{2}\Delta\varphi$	1
	$\psi_{-\Delta\varphi-1/2}^{\bar{1}} 0\rangle$	$\frac{3}{2}\Delta\varphi$	1
	$\psi_{-1/2}^{2,3} 0\rangle$	$\frac{1}{2}\Delta\varphi$	$\alpha$
	$\psi_{-1/2}^{2,3} 0\rangle$	$\frac{1}{2}\Delta\varphi$	$\alpha^2$

Fermionic states on $T^2 \times T^4/\mathbb{Z}_3$				
on $T^2$	state	mass	chirality	$\mathbb{Z}_3$
$\Delta\varphi = 0$	$ 0\rangle_R$	0	$L$	1
	$\psi_0^0\psi_0^1 0\rangle_R$	0	$R$	1
	$\psi_0^0\psi_0^2 0\rangle_R$	0	$R$	$\alpha$
	$\psi_0^0\psi_0^3 0\rangle_R$	0	$R$	$\alpha^2$
	$\psi_0^1\psi_0^2 0\rangle_R$	0	$L$	$\alpha$
	$\psi_0^1\psi_0^3 0\rangle_R$	0	$L$	$\alpha^2$
	$\psi_0^2\psi_0^3 0\rangle_R$	0	$L$	1
	$\psi_0^0\psi_0^1\psi_0^2\psi_0^3 0\rangle_R$	0	$R$	1
$\Delta\varphi \neq 0$	$ 0\rangle_R$	0	$L$	1
	$\psi_0^0\psi_0^2 0\rangle_R$	0	$R$	$\alpha$
	$\psi_0^0\psi_0^3 0\rangle_R$	0	$R$	$\alpha^2$
	$\psi_0^2\psi_0^3 0\rangle_R$	0	$L$	1

## D Chiral Spectra of Examples 2a and 2b

Chiral fermionic spectrum for example 2a										
	mult.	$SU(3) \times SU(2)_L \times SU(2)_R \times SO(8)$	$Q_A^1$	$Q_B^1$	$Q_B^2$	$Q_C^1$	$Q_C^2$	$Q_{B-L}$	$Q'$	$Q''$
$AB\alpha^0$	2	$(\bar{3}, 2, 1, 1)$	-1	1	0	0	0	1/3	5/3	1/4
	2	$(3, 1, 2, 1)$	1	0	1	0	0	-1/3	-5/3	1/4
$\alpha^1$	1	$(1, 2, 1, 8)$	0	-1	0	0	0	0	-1	-1/4
	1	$(3, 1, 2, 1)$	1	0	-1	0	0	-1/3	1/3	-1/4
$\alpha^2$	1	$(1, 1, 2, 8)$	0	0	-1	0	0	0	1	-1/4
	1	$(\bar{3}, 2, 1, 1)$	-1	-1	0	0	0	1/3	-1/3	-1/4
$AC\alpha^0$	2	$(3, 1, 1, 1)$	1	0	0	-1	0	-4/3	-2/3	-1/2
	2	$(\bar{3}, 1, 1, 1)$	-1	0	0	0	-1	4/3	2/3	-1/2
$\alpha^1$	1	$(1, 1, 1, 8)$	0	0	0	1	0	1	0	1/2
	1	$(\bar{3}, 1, 1, 1)$	-1	0	0	0	1	-2/3	2/3	1/2
$\alpha^2$	1	$(1, 1, 1, 8)$	0	0	0	0	1	-1	-0	1/2
	1	$(3, 1, 1, 1)$	1	0	0	1	0	2/3	-2/3	1/2
$BB'\alpha^0$	2	$(1, 2, 2, 1)$	0	1	1	0	0	0	0	1/2
$\alpha^1$	1	$(1, 1, 1, 1)$	0	-2	0	0	0	0	-2	-1/2
$\alpha^2$	1	$(1, 1, 1, 1)$	0	0	-2	0	0	0	2	-1/2
$CC'\alpha^0$	2	$(1, 1, 1, 1)$	0	0	0	-1	-1	0	0	-1
$\alpha^1$	1	$(1, 1, 1, 1)$	0	0	0	2	0	2	0	1
$\alpha^2$	1	$(1, 1, 1, 1)$	0	0	0	0	2	-2	0	1
$BC'\alpha^0$	2	$(1, 2, 1, 1)$	0	-1	0	-1	0	-1	-1	-3/4
	2	$(1, 1, 2, 1)$	0	0	-1	0	-1	1	1	-3/4
$\alpha^1$	1	$(1, 2, 1, 1)$	0	1	0	0	1	-1	1	3/4
$\alpha^2$	1	$(1, 1, 2, 1)$	0	0	1	1	0	1	-1	3/4

Table 5: Chiral fermionic spectrum for example 2a

Chiral fermionic spectrum for example 2b								
	mult.	$SU(3) \times SU(2)_L \times SU(2)_R \times SO(8)$	$Q_A^1$	$Q_B^1$	$Q_B^2$	$Q_C^1$	$Q_{B-L}$	$Q'$
$AB\alpha^0$	2	$(\bar{3}, 2, 1, 1)$	-1	1	0	0	1/3	1
	2	$(3, 1, 2, 1)$	1	0	1	0	-1/3	-1
$\alpha^1$	1	$(1, 2, 1, 8)$	0	-1	0	0	0	-1
	1	$(3, 1, 2, 1)$	1	0	-1	0	-1/3	1
$\alpha^2$	1	$(1, 1, 2, 8)$	0	0	-1	0	0	1
	1	$(\bar{3}, 2, 1, 1)$	-1	-1	0	0	1/3	-1
$BB'\alpha^0$	2	$(1, 2, 2, 1)$	0	1	1	0	0	0
$\alpha^1$	1	$(1, 1, 1, 1)$	0	-2	0	0	0	-2
$\alpha^2$	1	$(1, 1, 1, 1)$	0	0	-2	0	0	2
$BC\alpha^0$	2	$(1, 2, 1, 1)$	0	-1	0	1	-1	1
	2	$(1, 1, 2, 1)$	0	0	-1	-1	1	-1
$\alpha^1$	1	$(1, 1, 2, 1)$	0	0	1	-1	1	-3
$\alpha^2$	1	$(1, 2, 1, 1)$	0	1	0	1	-1	3

Table 6: Chiral fermionic spectrum for example 2b

## References

- [1] A. Sagnotti, ROM2F-87-25 *Talk presented at the Cargese Summer Institute on Non-Perturbative Methods in Field Theory, Cargese, France, Jul 16-30, 1987.*
- [2] J. Polchinski, Phys. Rev. Lett. **75** (1995) 4724 [hep-th/9510017](#).
- [3] G. Pradisi and A. Sagnotti, Phys. Lett. B **216** (1989) 59. J. Govaerts, Phys. Lett. B **220** (1989) 77. P. Horava, Nucl. Phys. B **327** (1989) 461. M. Bianchi and A. Sagnotti, Phys. Lett. B **247** (1990) 517. M. Bianchi and A. Sagnotti, Nucl. Phys. B **361** (1991) 519.
- [4] E. G. Gimon and J. Polchinski, Phys. Rev. D **54** (1996) 1667 [hep-th/9601038](#).
- [5] N. Arkani-Hamed, S. Dimopoulos and G. R. Dvali, Phys. Lett. B **429** (1998) 263 [hep-ph/9803315](#). I. Antoniadis, N. Arkani-Hamed, S. Dimopoulos and G. R. Dvali, Phys. Lett. B **436** (1998) 257 [hep-ph/9804398](#).
- [6] A. Dabholkar and J. Park, Nucl. Phys. **B472** (1996) 207 [hep-th/9602030](#).
- [7] E. G. Gimon and C. V. Johnson, Nucl. Phys. **B477** (1996) 715 [hep-th/9604129](#).
- [8] M. Berkooz and R. G. Leigh, Nucl. Phys. **B483** (1997) 187 [hep-th/9605049](#). J. D. Blum and A. Zaffaroni, Phys. Lett. **B387** (1996) 71 [hep-th/9607019](#). Z. Kakushadze and G. Shiu, Phys. Rev. **D56** (1997) 3686 [hep-th/9705163](#). G. Zwart, Nucl. Phys. **B526** (1998) 378 [hep-th/9708040](#). S. Förste and D. Ghoshal, Nucl. Phys. **B527** (1998) 95 [hep-th/9711039](#).

- D. O’Driscoll, [hep-th/9801114](#). G. Aldazabal, A. Font, L. E. Ibanez and G. Violero, Nucl. Phys. **B536** (1998) 29 [hep-th/9804026](#).
- [9] M. Cvetič, M. Plumacher and J. Wang, JHEP **0004** (2000) 004 [hep-th/9911021](#). G. Pradisi, Nucl. Phys. B **575** (2000) 134 [hep-th/9912218](#). B. Feng, Y. He, A. Karch and A. Uranga, [hep-th/0103177](#).
- [10] R. Blumenhagen, L. Görlich and B. Körs, Nucl. Phys. **B569** (2000) 209 [hep-th/9908130](#). R. Blumenhagen, L. Görlich and B. Körs, JHEP **0001** (2000) 040 [hep-th/9912204](#). S. Förste, G. Honecker and R. Schreyer, Nucl. Phys. B **593** (2001) 127 [hep-th/0008250](#).
- [11] T. Banks and L. Susskind, [hep-th/9511194](#). A. Sen, Class. Quant. Grav. **17** (2000) 1251. A. Lerda and R. Russo, Int. J. Mod. Phys. A **15** (2000) 771 [hep-th/9905006](#).
- [12] M. R. Gaberdiel, Class. Quant. Grav. **17** (2000) 3483 [hep-th/0005029](#).
- [13] C. Bachas, [hep-th/9503030](#).
- [14] C. Angelantonj, I. Antoniadis, E. Dudas and A. Sagnotti, Phys. Lett. B **489**, 223 (2000) [hep-th/0007090](#).
- [15] R. Blumenhagen, L. Görlich, B. Körs and D. Lüst, JHEP **0010**, 006 (2000) [hep-th/0007024](#). R. Blumenhagen, L. Görlich, B. Körs and D. Lüst, Fortsch. Phys. **49**, 591 (2001) [hep-th/0010198](#).
- [16] A. Hashimoto and W. I. Taylor, Nucl. Phys. B **503**, 193 (1997) [hep-th/9703217](#).
- [17] M. Berkooz, M. R. Douglas and R. G. Leigh, Nucl. Phys. B **480**, 265 (1996) [hep-th/9606139](#).
- [18] C. Angelantonj and A. Sagnotti, [hep-th/0010279](#).
- [19] R. Blumenhagen, B. Körs and D. Lüst, JHEP **0102**, 030 (2001) [hep-th/0012156](#).
- [20] L. E. Ibáñez, F. Marchesano and R. Rabadan, JHEP **0111**, 002 (2001) [hep-th/0105155](#). L. E. Ibáñez, [hep-ph/0109082](#).
- [21] R. Rabadan, [hep-th/0107036](#).
- [22] R. Blumenhagen, B. Körs, D. Lüst and T. Ott, Nucl. Phys. B **616**, 3 (2001) [hep-th/0107138](#). R. Blumenhagen, B. Körs, D. Lüst and T. Ott, [hep-th/0112015](#).
- [23] S. Förste, G. Honecker and R. Schreyer, JHEP **0106** (2001) 004 [hep-th/0105208](#).
- [24] M. Cvetič, G. Shiu and A. M. Uranga, Phys. Rev. Lett. **87** (2001) 201801 [hep-th/0107143](#). M. Cvetič, G. Shiu and A. M. Uranga, Nucl. Phys. B **615** (2001) 3 [hep-th/0107166](#). M. Cvetič, G. Shiu and A. M. Uranga, [hep-th/0111179](#).
- [25] G. Aldazabal, S. Franco, L. E. Ibáñez, R. Rabadan and A. M. Uranga, J. Math. Phys. **42**, 3103 (2001) [hep-th/0011073](#).
- [26] G. Aldazabal, S. Franco, L. E. Ibáñez, R. Rabadan and A. M. Uranga, JHEP **0102**, 047 (2001) [hep-ph/0011132](#).
- [27] D. Bailin, G. V. Kraniotis and A. Love, [hep-th/0108131](#).
- [28] G. Honecker, [hep-th/0112174](#).

- [29] H. Kataoka and M. Shimojo, [hep-th/0112247](#).
- [30] M. Bianchi, G. Pradisi and A. Sagnotti, Nucl. Phys. B **376** (1992) 365. M. Bianchi, Nucl. Phys. B **528** (1998) 73 [hep-th/9711201](#). E. Witten, JHEP **9802** (1998) 006 [hep-th/9712028](#). C. Angelantonj, Nucl. Phys. B **566** (2000) 126 [hep-th/9908064](#). Z. Kakushadze, Int. J. Mod. Phys. A **15** (2000) 3113 [hep-th/0001212](#).
- [31] M. R. Douglas and G. W. Moore, [hep-th/9603167](#).
- [32] Z. Lalak, S. Lavignac and H. P. Nilles, Nucl. Phys. B **559** (1999) 48 [hep-th/9903160](#).